Fall 12-17-2011

Exchange flows in an urban water body: Bayou St. John responses to the removal of flood control structures, future water elevation control, and water quality

Robin L. Schroeder
UNO, schroeder@ebsbiowizard.com

Exchange flows in an urban water body
Bayou St. John response to the removal of flood control structures, future water elevation control and water quality.

A Thesis

Submitted to the Graduate Faculty of the
University of New Orleans
in partial fulfillment of
the requirements for the degree of

Master of Science
in
Earth and Environmental Science
Geology

by

Robin Lynn Schroeder

B.S Texas A&M University in Galveston, 2005

December, 2011

Acknowledgements

I owe my deepest gratitude to everyone who helped me complete this study. Mostly, I would like to thank Dr. Ioannis Georgiou who taught me everything I know about numerical modeling and whose patience seems endless. His support and guidance were invaluable not only to completing this project but also in keeping my spirits high while working on it. I would also like to thank my other committee members, Dr. Alex McCorquodale and Dr. Martin O'Connell, for willingness to accommodate my needs and help in reviewing my work. Several people within the Earth and Environmental Sciences department were instrumental in field data collection including: Patrick Smith, Phil McCarty, and Dallon Weathers. The US Army Corps of Engineers, specifically George Brown in the Water Management Office provided additional data for modeling. I am very appreciative the rapid response and invaluable aid everyone mentioned above provided despite having to take time out of their busy schedules. I would also like to thank my family for their support and understanding during the long days and nights when I was not home and to my husband for taking up the slack while I was working on this project.

Table of Contents

List of Figures

List of Tables

Abstract

Bayou St. John, an urban water body extending south from Lake Pontchartrain, has two anthropogenic structures that regulate flow from the Lake . The City of New Orleans has plans to remove the inner control structure to improve water quality. Field and numerical methods used in this study show removing this structure increased water elevations throughout the Bayou but resulted in lower water elevation signal amplitudes that caused a lower tidal flow exchange from north to south. Bulk Richardson numbers showed mixing was inversely related to flow and the Bayou generally remains stratified. Resuspension of contaminated sediment could negatively impact the local ecology but predicted shear stress values did not reach a critical value (0.1 N/m^2) for resuspension. Removal of the waterfall structure will benefit Bayou St. John by decreasing energy losses from the Lake, however a more pronounced tidal signal from Lake Pontchartrain is required to flush the Bayou.

Keywords: Bayou St. John, contamination, shear stress, Bulk Richardson number, temperature, salinity, water elevation, waterfall structure

Chapter 1

1.1 Introduction

Bayou St John is a historically important waterway that lies along the eastern side of City Park in New Orleans, Louisiana (Figure 1). This Bayou has traditionally been a location for families and local fisherman to enjoy recreational activities and played an important role in the settlement of the city of New Orleans (Freiberg and Chase, 1980). Local businesses, residents and environmental advocacy groups, notably the Lake Pontchartrain Basin Foundation (LPBF, 2006) and the Bayou St. John Alliance, have made efforts to restore Bayou St. John to an ecologically healthy environment that the local community can enjoy for both educational and recreational benefit. Efforts have included dredging to decrease growth and subsequent decay of aquatic plant life, shoring the banks to reduce erosion (Ward, 1982), and restocking the Bayou with red drum (Brogan, 2010). The next phase of restoration is focused on improving water quality in the Bayou.

Flow into the Bayou is primarily from Lake Pontchartrain and to a lesser degree atmospheric input (precipitation) and storm water runoff (via bridges) from the surrounding residential neighborhoods. Flow between Lake Pontchartrain and Bayou St. John is restricted internally by two anthropogenic flood control structures. Sector gates located close to Lake Pontchartrain were initially designed to close only during storm events, however the gates generally remain closed. Sluice gates, on either side of the sector gates, however, have the ability to allow some flow and are operated manually. An older flood control structure, known as the waterfall structure, containing three culverts is located downstream (toward the Bayou) of the sector gates and is in poor condition. Two separate groups control water management (inflow and outflow) from the Bayou. These groups extract water from the Bayou for undisclosed time periods and flow. For example, City Park officials pump Bayou water into Lakes located within City Park to combat algae and hyacinth growth, to periodically flush the Lakes, and for other general water needs. The higher salinity water of Bayou St. John acts as an effective algaecide. The Sewerage and Water Board (SWB) controls two discharge valves in Bayou St. John that are opened in response to rising, or the anticipated rise, of water elevations in addition to sector gate control. These cumulative anthropogenic alterations have radically altered the normal hydrologic response within Bayou St. John.

Today the recreational benefits of Bayou St. John are minimal due to a reduction in quality and quantity of sport fish in the Bayou along with concerns for general water quality. Both

problems have been attributed to the flow restrictions caused by the waterfall structure and sector gates. Though there is little doubt aquatic wildlife migration is hindered by these anthropogenic structures, little is known about the internal hydrodynamics of the Bayou.

The local officials in the City of New Orleans government recently allocated funds to remove the culverts inhibiting flow at the waterfall structure, between the Bayou and the Lake. Removing the culverts will potentially increase the tidal exchange between the Bayou and Lake Pontchartrain. The resulting increase in tidal mixing and circulation is expected to alter water quality, which could potentially improve the ecological and environmental conditions of Bayou St. John. However, previous studies have identified the presence in high concentrations of toxic and otherwise harmful constituents harbored in the sediment of Bayou St. John (Mowat and Bundy, 2001). After removal of the waterfall structure, resuspension or general disturbance of this material from increased bed shear stress could have unforeseen negative consequences on the ecology and general water quality of the Bayou. This paper focuses on delineating the present tidal exchange between Bayou St. John and Lake Pontchartrain, identifying the governing controls of the exchange and through field data and use of numerical models predict future water quality and hydrodynamics.

1.2 Literature Review and Review of Numerical Methods

General hydrologic characteristics

Bayou St. John no longer acts as a natural waterway because the Bayou has restricted access to Lake Pontchartrain and no natural discharge. The flood control and water control structures limit flow, attenuate tidal fluctuations, and have stabilized Bayou St. John with respect to sediment flux, by establishing a low velocity environment. Removal of the waterfall structure, with a subsequent opening of the sector gates could change these conditions allowing for an increase in the amount of sediment into and out of the Bayou and potentially redistribute sediments within the Bayou itself.

Burk-Klienpeter, Inc. (2000) modeled the water flow from Lake Pontchartrain into Bayou St. John working on the assumption that water flow was controlled only at the sector gates to maintain Bayou water elevations at -0.8 m North American Vertical Datum, NAVD88. Hydraulic head differences were assumed to be the driving force for ecological habitat and high salinities were assumed to be the main requirement to maintain diversity in the Bayou (BKI, 2000). A full description of marine organism requirements and potential movement based on flow is given in this report. BKI (2000) used Hydraulic Engineering Center's Hydrologic Modeling System and River

Analysis System (HEC HMS and HEC RAS) to both model flow within subbasins of Bayou St. John, the City Park Lakes, and associated drainage canals and to model flow across the subbasins. The models did not consider meteorological conditions other than precipitation. The results from this modeling showed that though the city prefers to maintain the Bayou at -0.8 m NAVD88, the Bayou can support water elevations as high as 0.27 m NAVD88 with little impact to the surrounding area due to the levees surrounding the Bayou. The poor water quality in Bayou St. John is attributed to poor Lake water quality entering the standing body of water (BKI, 2000), rather than runoff from the urban interior. The waterfall structure was shown to block water flow into the Bayou when the sector gate valves were opened due to the rapid change in head and high degree of blockage within the waterfall culverts. Water backing up in the inlet upstream of the waterfall structure was shown to cause more than 1 m of water elevation difference between the inlet and north Bayou. BKI (2000) recommended removing the waterfall structure to improve flow into the Bayou from the Lake using recommended control strategies at the sector gates only. Opening discharge valves maintained by the SWB was also recommended to increase flow from north to south in the Bayou but was not modeled (BKI, 2000).

There are many modern examples showing the relationship between inlets and open bodies of water. Work et al. (2001) showed how a mesoscale model of a current dominated inlet with limited sediment transport under-predicted the amount of sediment deposited within the inlet, though the model accurately predicted the trend in the adjacent shoreline movement. Lake currents near the inlet to Bayou St. John have limited capacity to produce longshore sediment transport primarily due to local armoring of the adjacent shorelines along the Lake Pontchartrain shore and due to the relatively deep sections in the vicinity of these armored sections. The depth inhibits wave breaking and the generation of longshore transport of sands, although longshore currents are capable of transporting fine sediments. These fine sediments can be transported and deposited within the Bayou. Fixed or armored shorelines along inlets lead to deep and narrow geomorphologies when compared to inlets with erodible banks in order to accommodate the same tidal prism (van der Wegen et al., 2010) This indicates that Bayou St. John could experience erosion if the tidal prism or tidal flux is allowed to increase. Erosion will likely target soft shorelines compared to sections of the inlet and Bayou that are armored or stabilized with concrete mats, bulkheads and other shoreline protection measures. Bottom resuspension of sediments is due to the cumulative effect of wind driven waves and currents both of which are in effect during cold fronts (Stanev et al., 2009). Wave amplitudes create greater shear stress boundary conditions than currents alone and therefore have a greater impact on sediment re-suspension and transport

(Glenn and Grant, 1987). However, Bayou St. John is narrow with limited fetch and therefore currents may prove to be the dominant process controlling sediment transport. Storm induced waves can have a significant impact on sediment deposition and transport depending on their zone of intensity and duration (Ranasinghe and Pattiaratchi, 2003). Flow at the culmination of a storm could cause sediment redistribution by effectively flushing disturbed sediment from the Bayou, either through discharge or return flow to the Lake (Ranasinghe and Pattiaratchi, 2003). Increased flow after the removal of the waterfall structure could increase the impact these events have on Bayou St. John.

Lake Pontchartrain is a large, shallow Lake that is susceptible to large changes in water elevation due to wind-induced setup or set-down and barometric effects, all of which occur generally during storm events. These fluctuations directly impact water elevations in Bayou St. John. Storm surges from hurricanes have been observed to triple the tidal amplitudes and cause increased water elevations of over a meter lasting for several days (Li et al., 2010). Lake Pontchartrain has a small average tidal range of approximately 11 cm, which generally allows surface currents to be dominated by wind action (Stone et al., 1972). In 1996 a constant easterly wind led to setup from Lake Pontchartrain into the Amite River causing localized flooding (Hsu et al., 1997). Wind setup in shallow water bodies can balance tidal forcing if the tidal prism is small with strong predominant winds such as between two estuarine systems (Traynum and Styles, 2008). In Bayou St. John, wind from the south could potentially counter the tidal prism from Lake Pontchartrain, or retard tidal exchange. During stronger winds from the south, set-down in the Lake, accompanied by a small setup in the Bayou, could create pressure gradients that would result in increased exchange between these two water bodies. Historically however large storms in this area are generally associated with the stronger winds from the north following the passage of cold fronts. Without proper control, these storm events have the potential to steadily raise water elevations in Bayou St. John as was observed in the Amite River.

Contamination Sources and Documentation

Contamination and pollution has long been a concern for Louisiana waterways and Bayou St. John is no exception. Several studies have been conducted within New Orleans, LA and in Bayou St. John correlating trace metal contamination to runoff from roadways. Gonzales et al. (1997) and Wang et al. (2004) both show the main metals in Bayou St. John are lead and zinc. Additionally polycyclic aromatic hydrocarbons (PAH) have been found in high concentrations in the sediments (Mowat and Bundy, 2001; Wang et al., 2004). The ratio of different forms of PAH constituents have

a high correlation to incomplete automobile combustion and sampling shows both high PAH and higher metals concentrations at the south end of the Bayou. This can be attributed to higher vehicle traffic from run-off associated with the many bridges that cross Bayou St. John as well as from run-off directed to the south end of Bayou St. John from the interior of the city of New Orleans (Wang et al., 2004). A study conducted on Hurricane Katrina floodwater in New Orleans found that lead and arsenic levels were present in small quantities but above EPA drinking water standards (Pardue et al., 2005). Though the levels were not considered overly hazardous, the Katrina study shows many of the contaminants found in Bayou St. John can be attributed to accumulation of contaminated runoff (Pardue et al., 2005). Toxicity bioassays conducted in Bayou St. John also show much higher toxicity associated with sediment samples at the southern end of the Bayou than closer to Lake Pontchartrain (Mowat and Bundy, 2001). Temperature, salinity, dissolved oxygen, and conductivity were not found to be significantly different from north to south in the Bayou during 2009 field observations, however tagged red fish were not observed to travel south of I-610 (Brogan, 2010). This behavior may be linked to the heavily contaminated sediments found in the southern portion of the Bayou, reducing mixing conditions, and generally a lower velocity environment.

There is additional evidence suggesting some contaminants coming into Bayou St. John originate from Lake Pontchartrain (Boyd et al., 2004; McCorquodale et al., 2004). Trace metals, including lead, copper, and cadmium, are common constituents of re-suspended sediment samples taken from Lake Pontchartrain (Manheim et al., 1998). Lead and arsenic levels adsorbed to sediment in Lake Pontchartrain are above EPA criteria for clean soil and are consistent with long term accumulation (Dortch et al, 2008). Broken sewer lines due to subsidence (McCorquodale et al., 2001) allow raw sewage into the canals and waterways surrounding New Orleans including both Lake Pontchartrain and Bayou St. John. Fecal coliform are routinely discharged into Lake Pontchartrain along with storm water runoff gathered in New Orleans (Houck et al., 1989). Two discharge canals are located near Bayou St. John and field data and modeling of fecal coliform transport shows that concentration of these bacteria increases at the mouth of the inlet during discharge events and lasts for several days (McCorquodale et al., 2004; Carnelos 2003). Boyd et al. (2004) studied the concentration of raw sewage related chemicals in Bayou St. John and based on trends with rainfall concluded the source of these chemicals was most likely from Lake Pontchartrain. Furthermore, fecal coliform were shown to persist in sediments deposited along the south shore much longer than free bacteria in the water column (McCorquodale et al., 2004). Both sediment resuspended by wind-induced waves (List and Signell, 1996) and contaminated suspended sediment from New Orleans storm water discharge have the potential to be carried into

Bayou St. John. Previous studies have delineated the path of certain sediment bound contaminants (Chilmakuri, 2005). Flow into the Bayou could be regulated to avoid inflow during the peak transport of these and other associated contaminants (Boyd et al., 2004) and thereby minimize transport of contaminants into Bayou St. John. With these considerations, increased tidal mixing may produce benefits in terms of salinity, temperature and increased movement of marine organisms into and out of the Bayou that may outweigh the possible risks associated with Lake borne contamination.

Sediment Characteristics

Bayou St. John is an inlet to a Lake system and therefore has innumerable analogs in the modern world. Sand grain size in ebb-tidal deltas generally consists of coarse and medium sized grains responding to the high-energy wave and tidal action found at the mouth of inlets and have alternating flood and ebb sand morphologies (Fitzgerald et al, 2010). Wave orbital velocity, resulting shear stress from waves and currents, and grain size are important equilibrium factors in maintaining the depth and width of an inlet system (Gerritsen et al., 2003) and in determining distribution of sediments. Mowat and Bundy (2001) identified the north portion of Bayou St. John is dominated by sands and the southern portion is dominated by silts and clays corresponding to decreasing transport energy.

The majority of sediment in Bayou St. John and in Lake Pontchartrain are composed of silts and clays (Flocks et al., 2009), which generally contain large amounts of organic content, PAH, and metals (Mowat and Bundy, 2001). Resuspension of this material has the potential to negatively impact the local ecology. Once the sediment is suspended, transport distance is related to the viscosity of the water and the size of the sediment grain (Cheng, 1997) in conjunction with the forcing of the current (Glenn and Grant, 1987). Erosional properties of benthic materials are difficult to predict and direct measurement of these properties is outside the scope of this study. However, experiments conducted with SEDFLUME on poorly consolidated organic cores can be used as a guideline for probable erosional response to increased bed shear stress (McNeil et al., 1996). Additional data are available from Haralampides (2000) where the critical shear stress of Lake Pontchartrain bottom sediments was approximately 0.1 N/m^2 with an average porosity of 0.8. Sediment burial rate is negligible due to a low sediment accumulation rate and heavy bioturbation normally associated with Lake Pontchartrain benthic communities (Flocks et al., 2009).

Key Hypotheses

Hypothesis 1:The increased tidal mixing in Bayou St. John resulting from the removal of the "waterfall" structure will increase flushing, which will cause temperature and salinity values to more closely follow Lake Pontchartrain values.

Hypothesis 2: Removal of the "waterfall" structure will increase bottom shear stress leading to sediment resuspension, which will redistribute contaminated sediment in Bayou St. John.

Scientific Questions

The specific scientific questions to be answered in this study are:

1. How much energy is lost between Lake Pontchartrain and Bayou St. John?
2. How much energy will be recovered from removing the waterfall structure?
3. How will the energy recovered from the removal of the structure affect water elevations within Bayou St. John?
4. Will temperature and salinity gradients mimic Lake Pontchartrain in response to increased flow and resulting exchange from the Lake?
5. Will the increased flow re-suspend sediments within the Bayou potentially mobilizing toxic compounds?

Figure 1. The insets show the location of Bayou St. John in relation to the state of Louisiana and close-up aerial photographs of the sector gates and waterfall structure located in the inlet. The large image is an aerial photograph of Bayou St. John next to City Park and encompasses a portion of New Orleans, LA and Lake Pontchartrain. The legend details symbols that delineate locations of the different discharge control features, anthropogenic structures, and field data collection.

Objectives

The specific objectives of this study are as follows:

1. Develop a model to predict flow and water elevations between Lake Pontchartrain and Bayou St. John through the anthropogenic control structures.
2. Develop and calibrate a model to characterize the current hydrodynamics inside Bayou St. John.
3. Apply the different flow inputs to the model to identify possible changes in flow characteristics, primarily water elevation, shear stress, temperature, and salinity.
    a. Flow when the waterfall structure is removed with the sector gates closed.
    b. Flow if the sector gates remain open and the waterfall structure is removed.
    c. Flow if the sector gates are opened with the waterfall structure in-place
4. Use shear stress calculated by the model to analyze the potential for sediment resuspension in Bayou St. John.
5. Analyze the resultant flushing and tidal mixing with respect to salinity and temperature.

Chapter 2. Study Area and Significance

New Orleans and Lake Pontchartrain

New Orleans and the surrounding area receive approximately 61 inches of rain annually with an average temperature of 25.33°C in the summer and 14.78°C in the winter resulting in a humid, subtropical climate. Winds are seasonal with northwest winds dominating in the winter and southeast winds dominating in the summer. The average evaporation, estimated with pan evaporation, varies greatly by month (Fontenot, 2004) due to changes in temperature and humidity. Lake Pontchartrain is a brackish estuarine Lake that is approximately 1,630 km^2. During the winter, from approximately November to April, cold fronts periodically come across Lake Pontchartrain resulting in a hydrologic set-up at the connection of Bayou St. John to Lake Pontchartrain accompanied by precipitation and storm water runoff. The predictable nature of these storms generally triggers a response from the New Orleans Sewerage and Water Board to drain the Bayou and close the sector gates for an undetermined length of time to prevent excessive water elevations.

Bayou St. John

Bayou St. John is a brackish, natural water body that lies on the eastern side of City Park in New Orleans, LA (Figure 1). The Bayou receives water from Lake Pontchartrain from the north and this process is the primary driver for water level fluctuations in the Bayou. Anthropogenic operations in the inlet and within Bayou St. John control the range of water elevations locally to prevent flooding of surrounding neighborhoods. The geometry of the Bayou, and the location of these extraction locations from operations, separate the Bayou into two distinct hydrologic sections: the inlet near the north end of the Bayou, and the Bayou itself.

Inlet

The structure and physical description of the inlet to Bayou St. John from Lake Pontchartrain is complex due to extensive anthropogenic alterations. Potential flooding and gradual erosion along the banks of the Bayou led city officials with the help of the Army Corps of Engineers to completely redesign the inlet of Bayou St. John starting in the early 1960s. Today a sector gate controls flow from the Lake into a concrete channel approximately 360 m in length ending in what locals call the “waterfall”. The sector gate was built in 1982 and is located south of Lake Shore Dr. while the waterfall structure was built in 1962 and is located 15 m north of Robert

E. Lee blvd (Brogan, 2010; LPBF, 2006; Ward, 1982). The sector gates remain closed, however there are two sluice gates covered by a wire mesh on either side that allow water to enter the concrete channel even when the gates are at the closed position (Brogan, 2010). The waterfall structure is a dam containing three culverts equipped with butterfly valves. Two of these culverts are 1.5 m in diameter and one is 0.5 m in diameter (Ward, 1982). The culverts are presumably partially blocked with only two pipes open at approximately 1.5 and 0.6 m respectively (Brogan, 2010).

Bayou

Bayou St John is approximately 6 km long and varies in width from 210 m at its widest point to 61m wide further inland. Figure 1 shows the location of associated internal water control structures. Martinez et al. (2008) completed a partial hydrographic survey, which provides enough information to extrapolate the missing segments for this study. From this dataset the average water depth of the Bayou is approximately 2.5 m. Several internal water control structures regulate the water elevation of Bayou St. John. A gravity weir and two storm water pumps are used to extract water from Bayou St. John into small ponds located within City Park (LPBF, 2006). Two additional manual valves are located south of I-610 operated by the New Orleans Sewerage and Water Board to lower water levels in the Bayou. However the discharge from these locations is assumed to have minimal impact on the flow dynamics of the Bayou. Bayou St. John has 12 bridges, one walkway, and a railroad traversing its length, all of which create localized constrictions.

Historical Trends in Bayou St. John

Water quality parameters are characteristics of the water column that change in response to outside forces such as climate and precipitation. The LSU Agricultural Center has a historical database that captures the variability in water characteristics in Bayou St. John. Table 1 shows the range and average temperature, salinity, conductivity, depth, and dissolved oxygen recorded by the LSU Agricultural multi-parameter sondes in 2009 and 2010.

Lake Pontchartrain supplies brackish water to Bayou St. John through the inlet. In general, Lake Pontchartrain receives salt water from the Gulf of Mexico through Lake Borgne, and receives freshwater from the North shore from through tributaries that empty into Lake Pontchartrain as into Lake Maurepas. The Lake is more saline in the summer compared to winter (Haralampides, 2000) largely in response to reduce freshwater input, increased evaporation and saltwater flux

through tidal mixing with its connection to the Gulf. Bayou St. John also follows this trend (Table 1). At the north end of Bayou St. John, salinities are near 6 ppt in August and between 3 to 4 ppt in December. The observed salinity in the central section of the Bayou and towards the south end, show decreased salinity from August to December 2009, which may be attributed to an intermittent connection with Lake Pontchartrain and an increase in precipitation and associated run-off during cold fronts.

Table 1. LSUAgricultural Center Historical Data Summary for Bayou St. John (2009-2010)

	Temperature °C	Sp. Conductivity	Salinity ppt	Depth ft	% D.O.	D.O. mg/L
North Bayou St. John August to December 2009						
Maximum	29.72	11.15	6.36	8.48	105.20	8.97
Minimum	11.43	6.27	3.44	5.48	28.61	2.17
Average	21.65	9.59	5.39	7.19	65.20	5.76
South Bayou St. John August to December 2009						
Maximum	34.25	9.84	5.49	10.28	105.51	10.47
Minimum	5.51	2.99	1.54	4.97	34.82	2.74
Average	23.34	5.24	2.83	8.28	68.10	5.90
Middle Bayou St. John August to December 2009						
Maximum	30.65	9.6	5.36	9.52	102.53	
Minimum	11.35	6.27	3.44	1.89	65.81	
Average	21.85	8.35	4.66	7.16	88.12	
Middle Bayou St. John January to June 2010						
Maximum	33.36	6.47	3.54	8.66	97.85	11.55
Minimum	5.64	3.71	1.93	6.88	57.08	4.11
Average	20.88	4.89	2.62	7.95	80.50	7.38

The average water temperature in Bayou St. John in 2009 was approximately 20°C with a range from 34°C in the summer to 5°C in the winter. The southern end of Bayou St. John is narrower and not as deep as the north, and has less access to Lake Pontchartrain, which is effectively a large heat sink. This allows the temperatures at the south end of Bayou St. John to vary more rapidly than the temperature in the north. This data correlates with the salinity data showing the southern end of Bayou St. John is less buffered from environmental factors than the north.

It is assumed the LSU Agricultural multi-parameter sondes were originally placed at similar elevations, however local subsidence may have altered their positions relative to each other. The

middle of the Bayou had the largest range in water surface or depth above the sensor, however the average depth measured at all three locations was fairly similar between 2 and 2.5 m.

Dissolved oxygen concentrations vary from 8.97 mg/L in the north to above 11 mg/L in the south. A second data set shows the dissolved oxygen levels within Bayou St. John are general aerobic with observed values between 4 and 7 mg DO/L depending on the depth sampled (Smith 2011, unpublished data), which is an acceptable range for a natural waterway. Dissolved oxygen levels were not observed to have large fluctuations between the north and south Bayou.

Chapter 3. Methods

Field Studies

Objective of Field Studies

The purpose of the field studies was to characterize the physical and chemical properties of Bayou St. John that is not present or not described in previous datasets or studies, and provide data to aid in the development of boundary conditions and in the calibration of numerical models. Specifically, synchronous fluctuations in water surface at various locations along the length of the Bayou, accompanied by temperature and salinity data, collected using moored deployments were required for initial model conditions. Deployment in the inlet provided inflow data upstream of the waterfall structure for analysis of water surface elevations dominated by Lake Pontchartrain forcing and floodgate control. Deployments within the Bayou were used to calibrate the numerical model with respect to water surface elevation in order to analyze the hydrologic characteristics of Bayou St. John. Sediment characteristics derived from analysis of grab samples were conducted to supplement previous geophysical data reported by Mowat and Bundy (2001) to determine the potential for sediment redistribution.

Sediment samples were collected on December 6, 2011. The continuous water monitoring data were collected from December 10, 2010 to January 8, 2011 to capture a series of cold front storm events. These storms provided a large contrast in water elevation and also signify events where anthropogenic controls would be activated. Data collected during the field studies and from data reviews were later used as input to a numerical model to develop a generalized representation of Bayou St. John predicting general hydrologic relationships of temperature, salinity, and water elevation as well as predictive shear stress based on various inflow scenarios.

Field Methods

Grab samples of surface sediments in Bayou St. John were obtained using a ponar sampler deployed from a rowboat. The samples were collected in ziplock bags and transported to a geophysical testing laboratory located in Baton Rouge, LA. The coordinates of sediment samples are listed in Appendix A and sample locations are shown in Figure 1. Samples were analyzed using method ASTM D 422, which includes sieve analysis and a hydrometer test.

Pressure, temperature, and salinity variability were continuously monitored using three multi-parameter sondes model YSI 6600. The height of each sonde was measured from the depth sensor to the base of the mooring and used to calculate the total depth from pressure readings. One sonde was deployed at a mid-point between the floodgates and the waterfall structure in the inlet (33.25°N, 78.14°E) and the depth sensor was positioned 0.31 m above the bed. A second sonde was deployed just south of the waterfall structure (33.25°N, 78.13°E) and the depth sensor was positioned 0.28 m above the bed. A third sonde was deployed near the first set of SWB control valves (33.21°N, 78.11°E) and was positioned 0.33 m above the bed. The sondes were attached to weighted stands and placed towards the middle of the channel in each respective location. Each YSI sonde was equipped with probes for temperature, specific conductivity, conductivity, total dissolved solids, turbidity, salinity, and pressure. Discrete samples were collected every 10 minutes. The sondes were deployed from 12-11-2010 to 1-8-2011. The recorded dataset was used as input and validation for numerical modeling and to analyze the hydrologic characteristics of the Bayou.

Currents in Bayou St. John were obtained using a Nortek Aquadopp, 3-D acoustic Doppler current meter. The Aquadopp acoustic meter was in an inverted position (northeast, southwest, down) facing upstream (northeast) and collected single point samples every 6 minutes. The instrument samples at 2 MHz for 2 minutes every 6 minutes and reports an average velocity resulting from that burst. The Aquadopp meter was attached to a weighted stand opposite the YSI 6600 sonde located just south of the waterfall structure (33.25°N, 78.13°E) and collected data from 12-11-2010 to 12-20-2010.

Water surface elevations (relative to a common datum) of each field station were established using a Magellan dual magnitude GPS base station and receiver. The vertical accuracy of the base station is 0.020m and the horizontal accuracy is 1.5mm (0.0049 ft) over a distance of up to 1,500 m; this is approximately 3 mm over a 1km survey distance. These elevations were collected while YSI sondes were deployed in the Bayou to provide a direct correlation between water elevation and depth. Using measured elevations collected using DGPS and survey methods, the recorded pressures were converted to a unified and common datum (NAVD 88). This water surface adjustment ensured that all data collected were referenced to the same datum, in order to obtain a direct measure of energy through the constricted section, and to better describe the dynamics of the Bayou.

Several data sets have previously been recorded and are readily available from local sources for additional validation and simulations. Water elevations for Lake Pontchartrain are collected hourly

by the US Army Corps of Engineers at two pumping stations located at London Avenue Canal and Orleans Outfall Canal that are juxtaposed on either side of the inlet to Bayou St. John (www.rivergages.com). Wind direction, wind speed (m/s), temperature (C), salinity (ppt), and pressure (mb) affecting Lake Pontchartrain during the field studies was collected from a weather station site monitored by the Louisiana Universities Marine Consortium (www.lumcon.edu). The LSU Agricultural Center has three continuous monitoring stations in the Bayou that collect depth, temperature, pressure, salinity, specific conductivity, and dissolved oxygen approximately every half hour. These data are available at: http://www.ysieconet.com/public/WebUI/Default.aspx?hidCustomerID=200. Another deployment to qualify water level dynamics over time was conducted by Schindler (2009), where an attempt to correlate changes in water levels, temperature, and salinity to wind and precipitation patterns over a two-month period. To date, no further analysis has been completed using either data set to study a dynamic response of the Bayou to similar events.

Numerical Modeling

Hydrodynamic models were used to understand the tidal mixing and potential changes in shear stress in Bayou St. John related to changes made at the inlet. To reduce complexity near model boundaries and to overcome model limitations, a 1-D energy-equation with minor losses was used to relate the corresponding water level changes across the restricted zone from the floodgates to the culverts. The interior of Bayou St. John will be modeled using a three-dimensional hydrodynamic model with a computational grid starting at the waterfall structure and encompassing the geometric and bathymetric variability of the Bayou. Bridges are represented as localized restrictions to flow. The model will be driven by results from either the 1-D equations or by observed field water elevations and by meteorological forcing (wind stress, heat flux, precipitation and evaporation). Table 2 summarizes the model simulations and the objective of each simulation. Specifics regarding the model and simulations are discussed in Chapter 4. Model results were calibrated and validated using the field data collected at the moored locations.

Table 2. Simulation table describing model scenarios, objectives, input details, and numerical methods for hydrodynamic modeling.

Simulation	Objective	Details	Methods
1. Calibration	Characterize the present day hydrodynamics in Bayou St. John	Forced with 1-D model using restricted zone field data	1-D model ECOMSED
2. Opening flood gates with waterfall in place	Characterize aspects of the waterfall structure	Forced with 1-D model using Lake Pontchartrain field data	1-D model ECOMSED
3. Removing waterfall with sector gates closed	Characterize the anticipated future hydrodynamics	Forced with restricted zone field data	Field Data ECOMSED
4. Open inlet- no restrictions	Characterize the potential water elevations of an unprotected Bayou	Forced with Lake Pontchartrain field data	Field Data ECOMSED

Model Skill Assessment

Several statistical methods were used to compare the time dependent datasets between observed and predicted values. The predicted values from the 1-D model are all scalar and therefore can be directly compared or correlated. Additional statistical methods were used to compare model results to observations. The root mean error (RME), root mean square error (RMSE), and index of agreement (d) (Willmott et al., 1985) compare observed (O) time dependent values to the predicted (P) values of the model then return an average fit value. For RME and RMSE, a value close to 0.0 indicates a good fit. The value of RME and RMSE will give an indication of deviation between observed and predicted values. The index of agreement measures the amount of agreement between time dependent responses. A d value closer to 1.0 indicates a better fit. The equations used have the following form:

$$RME = \frac{\sum_{n}^{i} |O_i - P_i|}{n} \quad \textbf{(1)}$$

$$RMSE = \sqrt{\frac{\sum_{n}^{i} |O_i - P_i|^2}{n}} \quad \textbf{(2)}$$

$$d = 1 - \left(\frac{\sum_{n}^{i} |P_i - O_i|^2}{\sum_{n}^{i} (|P_i - \overline{O}| + |O_i - \overline{O}|)^2} \right) \quad \textbf{(3)}$$

The model skill assessment used temperature, salinity, and water elevations at the north and south field observations sampled by the deployments. Additionally, a transect was extracted across the width of the Bayou at each of the listed locations in Table 3. The transects for each of these locations are shown in Figure 2 as panels. Table 3 describes the transect locations, discrete time segment the transects represent, and number of equidistant points extracted from the model along each transect. Field data were statistically compared to predicted values.

Table 3.Transect description including location, time segment, and number of points

Name	Transect Location	Time at which analysis was carried out (model simulation hour)	Number of points across Bayou width
A.	North Transect	40, 80, 180	20
B.	Mid Transect	40, 80, 180	20
C.	South Transects	40, 80, 180	20

Hydrologic Analysis of Simulations

Results from the hydrodynamic model simulations were analyzed for changes in free water surface elevation, shear stress, bottom and surface temperature, bottom and surface salinity, mixing, and tidal flow. Tidal exchange flow and mixing potential were assessed at three locations in the Bayou as described in Table 3 for instantaneous averages and as time dependent variables at the same locations. Mixing was evaluated by assessing the potential for the Bayou to produce stratification based on surface to bottom salinity and temperature gradients. The bulk Richardson number (Ri_L) approximates the impact of freshwater induced buoyancy on mixing. For this study the formulation of RiL suggested by Uncles and Stephens (2011) was used and has the following form:

$$Ri_L = gh\Delta\rho / \left(\rho U^2\right) \quad \textbf{(4)}$$

where ρ is the density of water, Δρ is the density gradient, h is the local water depth, and U is the depth-averaged velocity at that location.

Density was calculated used an equation of state for uniform ocean properties as follows:

$$\rho - \rho_o = -\bar{a}\left(T - T_o\right) + \bar{b}\left(S - S_o\right) + k_p \qquad \textbf{(5)}$$

where the temperature constant is 0.15 kg/m^3 per °C, the salinity constant is 0.78 kg/m^3 per ppt, the density constant is 4.5x10^{-3} kg/m^3 per decibar, initial density is 1027 kg/m^3, initial temperature is 10°C, and initial salinity is 35 psu. Instantaneous model predictions for temperature and salinity were used. The pressure effect on density was ignored in the evaluation of density given the shallow nature of the Bayou.

Tidal exchange flow was characterized by analyzing each transect described in Table 3 for instantaneous velocity and flow. Local velocity is calculated by the hydrodynamic model and flow is derived by integration of the velocity field over the area of the transect. Additionally, instantaneous flow, bulk Richardson number, and shear stress were also evaluated at these locations as time dependent variables. A loss of velocity or flow indicates mixing limitations from Lake Pontchartrain into Bayou St. John and within Bayou St. John from north to south.

Shear stress was evaluated at each transect described in Table 3 to determine the maximum value achieved as a result of changes made to the inlet of Bayou St. John and during sensitivity testing. A critical value of 0.1 N/m^2 (Haralampides, 2000) was used to evaluate the potential for sediment resuspension. The drag coefficient, C_d, is based on streamflow alone and was set at 0.01 after Mariotti et al. (2010). Density was calculated as an average using predicted salinity and temperature values at each location using an equation of state. The shear stress equation has the form of:

$$\tau_b = \rho C_d V^2 \qquad \textbf{(6)}$$

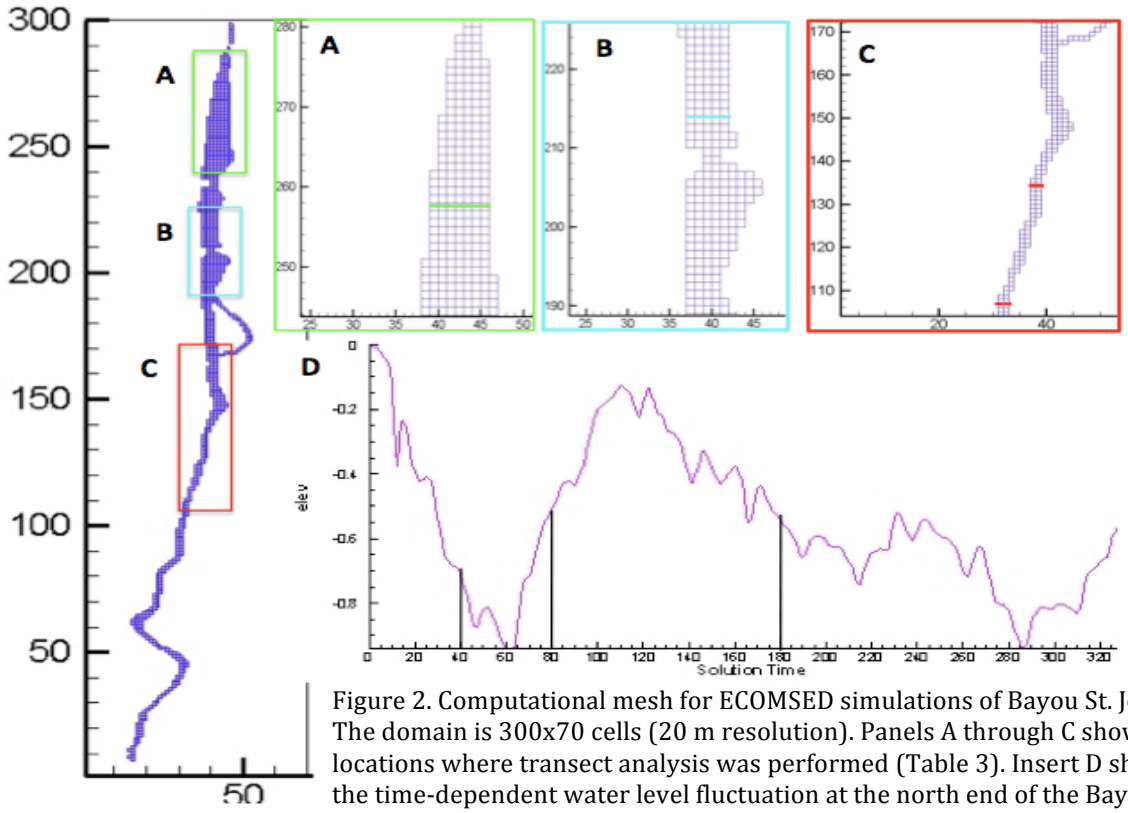

Figure 2. Computational mesh for ECOMSED simulations of Bayou St. John. The domain is 300x70 cells (20 m resolution). Panels A through C show locations where transect analysis was performed (Table 3). Insert D shows the time-dependent water level fluctuation at the north end of the Bayou and the solid black lines show the time at which analysis was performed.

Chapter 4. Numerical Modeling

Description of 1-D Numerical Methods:

Flow entering Bayou St. John from Lake Pontchartrain is complex due to multiple changes in channel size and flood control structures. To reduce complexity of the final hydrodynamic model of Bayou St. John, this upstream segment was simplified by treating the water fall structure as a boundary defined by a series of one-dimensional equations driven with field data collected upstream of the waterfall structure. The 1-D model assumes the stream-wise flow in the inlet is balanced by a non-linear bottom friction, which is a good approximation for long inlets as seen in Bayou St. John (Hench et al., 2002). The time period considered for the 1-D model captures a cold front induced amplitude in water elevation and maintains Lake Pontchartrain water elevations above the inlet and inlet water elevations above Bayou St. John. Stream-flow equations were used to characterize energy losses through the inlet during this time period. The geometry of the upstream segment of Bayou St. John along with a description of variables used in the one-dimensional model is available in Figure 3. Lake Pontchartrain and associated variables are termed Zone 1. The restricted zone, termed Zone 2, refers to the segment of flow through the concrete channel leading to Bayou Saint John located downstream of the sector gates and upstream of the waterfall structure. Zone 3 covers an expansion in the restricted zone channel immediately upstream of the waterfall structure. Flow through the culverts in the waterfall structure is associated with Zone P and Zone 4 is Bayou St. John.

Flow into the restricted zone from Lake Pontchartrain is unknown due to several complicating variables. The flow from Lake Pontchartrain crosses a mobile sand bar, a transition in channel size, and flows through sluice gates as part of the sector gates structure located near the mouth of the inlet. The mobility of the sand bar and operation of the sector gates is difficult to predict and introduces unnecessary complication to the proposed model and difficulty in establishing accurate boundary conditions. The water surface elevation of Lake Pontchartrain and the water surface elevation in the restricted zone are known from fieldwork and collected datasets. At least two full cold fronts were captured in these datasets. Lake Pontchartrain observed water surface elevations showed rapid responses to these weather changes in addition to maintaining a tidal response. In contrast, the field data in the restricted zone displays an attenuated response indicating dissipation that cannot be accounted for with a single friction term. The restricted zone is bounded on both sides by high levees. These structures prevent run-off from storm events from

entering the restricted zone and greatly decrease ability of wind to directly impact water in the restricted zone. These considerations among others prevent the one-dimensional model from accurately predicting the water surface elevation in the restricted zone using Lake Pontchartrain water surface elevations. Therefore the assumption is made that the water surface elevation inside the restricted zone will emulate the water elevation of Lake Pontchartrain if the sector gates are opened, i.e. frictional dissipation is assumed to be small relative to that presently imposed by water control structures.

Flow in the restricted zone between the sector gates and the waterfall structure is determined by gravity driven flow from Lake Pontchartrain and can be determined using Manning's equation.

$$Q=(1/n)\ AR^{2/3}S_o^{1/2} \quad \textbf{(7)}$$

Manning's n is set at 0.025 from a roughness table (rubble in cement) (Roberson et al., 1988). The slope is assumed to be very small, 0.0002, from Lake Pontchartrain to Bayou St. John. Field data water surface elevations inside the restricted zone were used as the boundary condition of the 1-D model to calibrate the culvert constants in the waterfall structure. The restricted zone expands in a wedge transition immediately upstream of the waterfall structure. The continuity equation can be used to determine the velocity within the transition zone.

$$V_2A_2 = V_3A_3 \quad \textbf{(8)}$$

To determine the water surface elevation immediately upstream of the culverts the transition equation can be used replacing head loss with an expansion term:

$$\alpha_2 \frac{V_2^2}{2g} + z_2 = \alpha_3 \frac{V_3^2}{2g} + z_3 + K_e \frac{V_2^2 + V_3^2}{2g} \quad \textbf{(9)}$$

The two unblocked culverts are both 1.5 m in diameter and 6.3 m long. Both culverts are blocked by butterfly valves that are rusted closed at different angles. The head loss through the culverts can be equated to the water surface elevation change across the waterfall structure:

$$z_3 - z_4 = 0.5\frac{V_P^2}{2g} + \frac{V_P^2}{2g} + K_L \frac{V_P^2}{2g} + L_P\left(\frac{n}{D^{5/3}}\right)^2 \quad \textbf{(10)}$$

K_L is a friction term that takes the butterfly valves into account. The K_L value can range from below 1 to above 300 based on the degree that the valve is closed (Chaiworapeuk, 2007). D is the diameter of the culverts.

From this series of one-dimensional equations the water surface elevation of Bayou St. John and the velocity exiting the waterfall culverts can be determined using the water surface elevation just inside the sector gates.

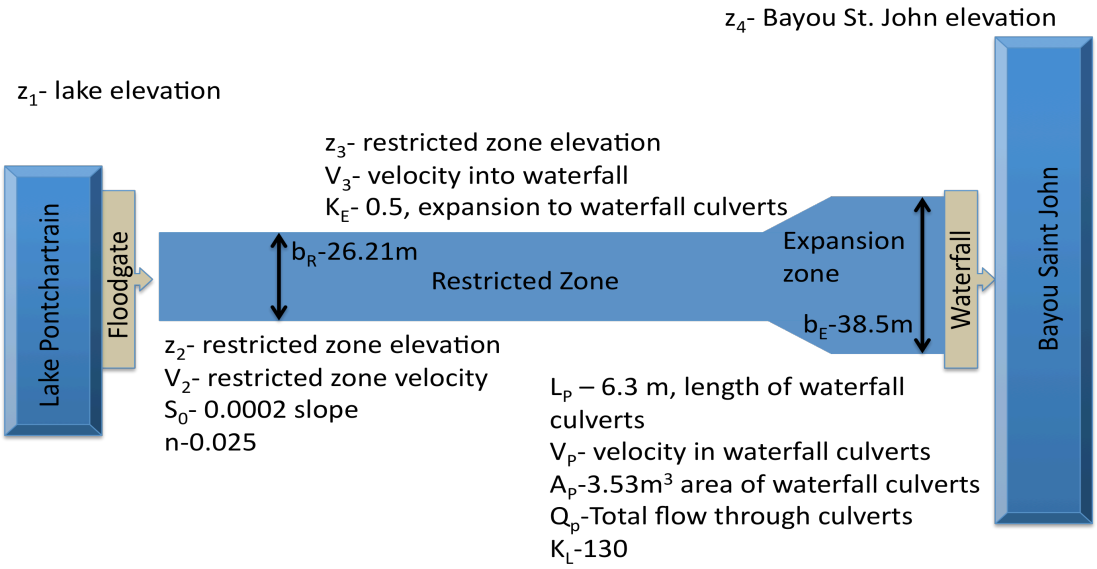

Figure 3. Schematic representation of the inlet into Bayou St. John detailing both anthropogenic structures, local geometry of the channel, and constants determined through field methods and calibration of the 1-D model.

Description of ECOMSED

The model selected to assess circulation within Bayou St. John is the Estuarine, Coastal and Ocean Modeling System with Sediments (ECOMSED) developed within Hydroqual Inc. from an earlier form originally developed by Blumberg and Mellor (1987). The Estuarine, Coastal, and Ocean Model with Sediment (ECOMSED) is a three dimensional model that has previously been used to model several physical aspects of circulation within Lake Pontchartrain including wind-driven circulation without buoyancy forcing (Signell and List, 1997), fate and transport of pathogenic organisms in the north and south shores of the Lake (Chilmakuri 2005), and to study cohesive sediment dynamics with spatial variability in response to frontal weather using satellite moderate spectrometer data (Georgiou et al.2007). For additional examples outside Lake Pontchartrain, refer to the ECOMSED manual (Hydroqual, 2002).

ECOMSED is a 3-D hydrodynamic and transport model designed to simulate several hydrologic parameters including dynamic water elevations, temperature, salinity, and sediment

transport over a specified time frame. ECOMSED uses the finite control volume principle and has a two-mode solution pathway. External, non-linear, horizontal transport of the overall movement of water is first calculated using short time scales of tidal and wind forcing while the second set of equations solves the processes of vertical velocity shear, and internal vertical mixing in large time steps with a turbulence closure scheme. The program is composed of modules that can be activated or deactivated dependent on the desired output. A three dimensional model was chosen in order to obtain the best estimate of bottom shear stress on potential sediment resuspension. The relative simplicity of the system minimizes computational requirements and allows the use of a 3-D model within a reasonable time frame. This model is fairly robust in both hydrologic and sediment transport schemes, however the model is limited in this application by the small spatial size of the Bayou. Only short time periods can be modeled to prevent artificial boundary responses from becoming significant (Blumberg and Mellor, 1987). Ramping is required to slowly adjust the dynamic water elevations due to input water elevation and meteorological forcing in order to avoid abrupt adjustments, which could cause some cells to dry. ECOMSED is unable to adjust for the sequential drying and wetting of cells, therefore a minimum depth is set in the model for each simulation such that no drying occurs.

ECOMSED solves for velocity in three dimensions, temperature, salinity, and internal vertical mixing using a turbulence closure scheme. The model is designed for an orthogonal Cartesian mesh, as was used here, but can be modified for curvilinear plots. Temperature and salinity are treated as conservative elements transported using changes in density based on the parameter values (p,T) and vertical eddy diffusion from turbulent mixing. The total depth was dicretized into sigma (σ) levels capable of deforming to follow localized bathymetry by Mellor and Yamada (1974). Sigma levels are fluid in vertical depth allowing them to constrict or expand to follow local bathymetry.

The basic ***Continuity Equation*** states transport of water across a cell volume at any given time will change the free water elevation in that column of cells.

$$\frac{\partial \eta}{\partial t} + \frac{\partial UD}{\partial x} + \frac{\partial VD}{\partial y} + \frac{\partial \omega}{\partial \sigma} = 0 \qquad \textbf{(11)}$$

where η is free water surface, U is horizontal velocity in the x direction, t is time, V is horizontal velocity in the y direction, ω is vertical velocity at σ, x is the east direction, σ is the discrete vertical zone, y is the north direction, and D is depth.

The ***Reynolds averaged momentum Equations*** describe the magnitude of flow across the cell on the left hand side of the equation and internal turbulent mixing in the cell on the right hand side of the equation. The relationship describes horizontal flow in the x and y directions as the sum of the magnitude of the U and V entering vectors as they change with time. Coriolis forces minimize flow by pulling water away from the direction of flow (x, opposite for y) and the weight of the water column (density). Horizontal flow is solved independently of vertical flow to allow water surface elevation changes. Potential density of the cell is based on the predicted temperature and salinity at atmospheric pressures, which is used to create baroclinic levels that can be mixed vertically in the turbulence closure scheme.

$$\frac{\partial UD}{\partial t}+\frac{\partial U^2D}{\partial x}+\frac{\partial UVD}{\partial y}+\frac{\partial U\omega}{\partial \sigma}-fVD+gD\frac{\partial \eta}{\partial x}=\frac{\partial}{\partial \sigma}\left(\frac{K_M}{D}\frac{\partial U}{\partial \sigma}\right)\frac{gD^2}{\rho_o}\frac{\partial}{\partial x}\int_\sigma^0 \rho d\sigma+\frac{gD}{\rho_o}\frac{\partial D}{\partial x}\int_\sigma^0 \sigma\frac{\partial \rho}{\partial \sigma}d\sigma+F_x \quad \textbf{(12)}$$

$$\frac{\partial VD}{\partial t}+\frac{\partial UVD}{\partial x}+\frac{\partial V^2D}{\partial y}+\frac{\partial V\omega}{\partial \sigma}+fUD+gD\frac{\partial \eta}{\partial y}=\frac{\partial}{\partial \sigma}\left(\frac{K_M}{D}\frac{\partial V}{\partial \sigma}\right)\frac{gD^2}{\rho_o}\frac{\partial}{\partial y}\int_\sigma^0 \rho d\sigma+\frac{gD}{\rho_o}\frac{\partial D}{\partial y}\int_\sigma^0 \frac{\partial \rho}{\partial \sigma}d\sigma+F_y \quad \textbf{(13)}$$

$$\frac{\partial \Theta D}{\partial t}+\frac{\partial \Theta UD}{\partial x}+\frac{\partial \Theta VD}{\partial y}+\frac{\partial \Theta \omega}{\partial \sigma}=\frac{\partial}{\partial \sigma}\left(\frac{K_H}{D}\frac{\partial \Theta}{\partial \sigma}\right)+F_\Theta \quad \textbf{(14)}$$

$$\frac{\partial SD}{\partial t}+\frac{\partial SUD}{\partial x}+\frac{\partial SVD}{\partial y}+\frac{\partial S\omega}{\partial \sigma}=\frac{\partial}{\partial \sigma}\left(\frac{K_H}{D}\frac{\partial S}{\partial \sigma}\right)+F_S \quad \textbf{(15)}$$

where f is the Coriolis factor using a β–plane, ρ is density at coordinates (x,y,z,t), g is gravitational density, ρ_0 is the reference density, F_xi s internal turbulence in the x direction, F_y is internal tubulence in the y direction, K_M is the vertical eddy for diffusivity of turbulent mixing, d is depth of the zone at coordinates (x,y,t), θ is temperature (°C), K_H is a coefficient for mixing, S is salinity (ppm), F_θ is internal heat flux, and F_S is internal mixing of salinity.

Kinetic turbulence is also a component of momentum and internal frictional forces Macroscale turbulence relates turbulence across multiple cells to define the zone of turbulent mixing. The values of K_M and K_H are solved using a closure scheme developed by Mellor and Yamada (1982) using the kinetic energy of turbulence, $q^2/2$, and the distance over which the turbulence is distributed (l). Turbulence at a particular depth is modified by the magnitude of mixing of flows in the U, V, and ω directions, heat flux, and salinity mixing. The terms F_x and F_y are defined as follows:

$$F_x \equiv \frac{\partial D\hat{\tau}_{xx}}{\partial x} + \frac{\partial}{\partial y}\left(D\hat{\tau}_{yx}\right) \quad \textbf{(16)}$$

$$F_y \equiv \frac{\partial D\hat{\tau}_{yy}}{\partial y} + \frac{\partial}{\partial x}\left(D\hat{\tau}_{xy}\right) \quad \textbf{(17)}$$

where the shear forces are associated with the magnitude of vectors.

The terms F_ℓ, F_q, F_S and F_Θ can be solved with the below equation.

$$F_{\theta_i} \equiv \frac{\partial D\hat{q}_x}{\partial x} + \frac{\partial D\hat{q}_y}{\partial y} \quad \textbf{(18)}$$

The model is limited by the free water surface, bottom bathymetry and wall geometry. At the bottom and lateral boundaries, salinity and temperature are set to zero. A free slip boundary is used at lateral boundary conditions. Bottom shear stress is calculated using a bottom roughness term, z_0.

ECOMSED initial conditions

The initial conditions for the Bayou St. John model include bathymetry, initial water depth, temperature, and salinity. Initial water elevation in Bayou St. John begins at 0m NAVD88 across all nodes (ie model starts from rest), which is the same datum as the bathymetry (Matrinez et al, 2008). An outline for Bayou St. John was extracted from Google Earth™ then incorporated into Tecplot™, a graphical interface, to develop the computational mesh for ECOMSED. An orthogonal Cartesian mesh of 70 cells by 300 cells with cell spacing of 20 UTM meters defined the study area as shown in Figure 2. Some areas of Bayou St. John are more restricted than others due to bridge crossings, which limited the number of nodes allowed in the channel. These geographical restrictions were artificially enlarged to reduce apparent friction in the model, produced by a combination of a low number of cells and the known stair-stepping effect. However, minor changes to the channel size are not expected to bias the model because the majority of the restricted areas are in the southern portion of the Bayou where flow is expected to be small. Depths were assigned to each node based on bathymetric data from Martinez et al. (2008) given in NAVD88. The model depth was adjusted for each simulation to the first elevation at the northern boundary condition to minimize the amount of ramping time used in the model, and to ensure model stability. The cold fronts captured by the field data encompass large variations in the water elevations in Bayou St.

John, which cause some shallow portions of the Bayou to completely drain. This situation cannot be simulated with ECOMSED because the model will not allow cells to dry and become wet again. To prevent the model from becoming unstable and to capture as much of the cold front as possible, the minimum depth of Bayou St. John was set to 2.0 m. Six vertical levels, or sigma levels, were assigned to Bayou St. John distributed at even intervals. Sediments were assigned a "mud" designation indicating the sediments are cohesive with an estimated roughness of 0.001 m, a drag coefficient of 0.0018, and a minimum friction of 0.025, which is a reasonable assumption given previous studies with ECOMSED, other estuarine studies (Uncles and Stephens, 2011), and the known characteristics of sediment in Bayou St. John. Initial temperature and salinity were set to 12.7°C and 3ppt (from observations from this study) and were spatially constant (same value was used for all nodes).

A narrow channel was added to the northernmost section of the grid defining Bayou St. John to represent the inlet. The channel was defined as two cells wide with a constant depth of 2.0 m and extended from the north end of the Bayou to the edge of the domain.

ECOMSED boundary conditions

The simulation period was from December 11 to December 25, 2010. Boundary conditions for this model application include atmospheric forcing and a tidal open boundary to the north with associated water elevation, temperature, and salinity. The relatively small size of the study area allows climatic conditions to be spatially constant (but time-dependent). Meteorological variables used for boundary conditions included variable heat flux, wind speed, wind direction, (Lumcon.com) and monthly mean precipitation evaporation rates from Fontenot (2004). All meteorological forcing was reduced by 90% assuming the local topography and neighborhoods provide sheltering. Surface water elevation observed at the north end of Bayou St. John was used for the calibration assuming the water elevation is associated with energy losses through the waterfall structure. Temperature and salinities associated with the restricted zone field observations were applied to the northern open boundary rather than field observations associated with the north end of Bayou St. John. These values were used initially in preparation for comparison of tidal flow exchange and mixing among later simulations once the waterfall structure is removed. Temperature and salinity were defined as time-dependent quantities at the northern open boundary.

ECOMSED Simulations

To test the hypothesis simulations three and four were completed as laid out in Table 3. The second simulation listed in Table 2 was not assessed because the 1-D model failed to reproduce the observed water elevations in Bayou St. John.

The comparison of the calibration with the third simulation where the waterfall structure is removed is used to test the questions: how will energy recovered from the removal of the structure affect water elevations within Bayou St. John? and how much energy is lost between Bayou St. John and Lake Pontchartrain? The study was initiated because the waterfall structure will be removed specifically to increase water quality and ecological health of the Bayou. This simulation will directly test the changes in hydrologic characteristics based on this future condition.

The comparison of the calibration with the fourth simulation where both the waterfall is removed and sector gates are open is used to test the question: will temperature and salinity gradients mimic Lake Pontchartrain in response to increased flow and resulting exchange from the Lake? Increased operation, i.e. routinely opening, the sector gates has been suggested by other studies (BKI, 2000) to increase flushing of the Bayou with respect to salinities. This simulation will directly test this recommendation to analyze changes in water quality with respect to both temperature and salinity.

All simulations will be used to test the question: will increased flow re-suspend sediments within the Bayou potentially mobilizing toxic compounds? Contamination from sediment resuspension is a concern due to the high level of contamination previously found in the Bayou (Mowat and Bundy, 2001). Mobilization of these sediments will both release dissolved contaminants in the pore space of the sediments as well as introduce contamination to otherwise healthy parts of the Bayou once the sediment is redistributed. All simulations will be used to test the potential for resuspension due to shear stress in order to relate shear stress values to water elevation forcing at the inlet.

Chapter 5. Results

Results of Field Activities

Geophysical and Sediment Contamination Analysis

The distribution of sediments is a function of distance from the mouth of the inlet. The sediment mean grain size diameter decreases with increasing distance from the north. Figure 4 shows the sediment grain analysis and contamination data in comparison to bathymetry in Bayou St. John. The field results coupled with Mowat and Bundy (2001) sediment data shows the north end of Bayou St. John receives a fair amount of sand, most likely from Lake Pontchartrain. The deeper channels of Bayou St. John towards the middle of the Bayou have higher sand percentages than the shores where quiescent settling zones allow clays and silts to dominate the bed layer. Most transport energy seems to dissipate past Harrison Avenue as shown by the rapidly decreasing percentage of sand in samples further south. South of I-610, bottom sediment samples are dominated by clays and silt and are black and oily appearance and, according to Mowat and Bundy, (2001) contain high amounts of metal and PAH contaminants. PAH contaminants are generally concentrated in the southern end of Bayou St. John and are attributed to roadway runoff (Mowat and Bundy, 2001, Wang et al., 2004) while the north end of Bayou St. John has low to non-detect concentrations of PAH. The concentration of metals is also higher in the south, however metal concentrations in the north remain relatively high unlike PAH. A portion of the metals contamination is most likely derived from Lake Pontchartrain in addition to runoff. Table 4 gives a brief overview of the data collected by Mowat and Bundy (2001) relative to contamination guidelines developed by the Environmental Bureau of Investigation in Canada based on levels set by the Ministry of Environment and bioassays (2011). The samples SS-2 and SS-5 were collected in more shallow regions of the Bayou and contained shells, evidence of a benthic community, however no shells were recovered in samples south of I-610. The lack of an established benthic community in a historically natural inlet system is strong evidence that the accumulated contamination has severely degraded the ecosystem.

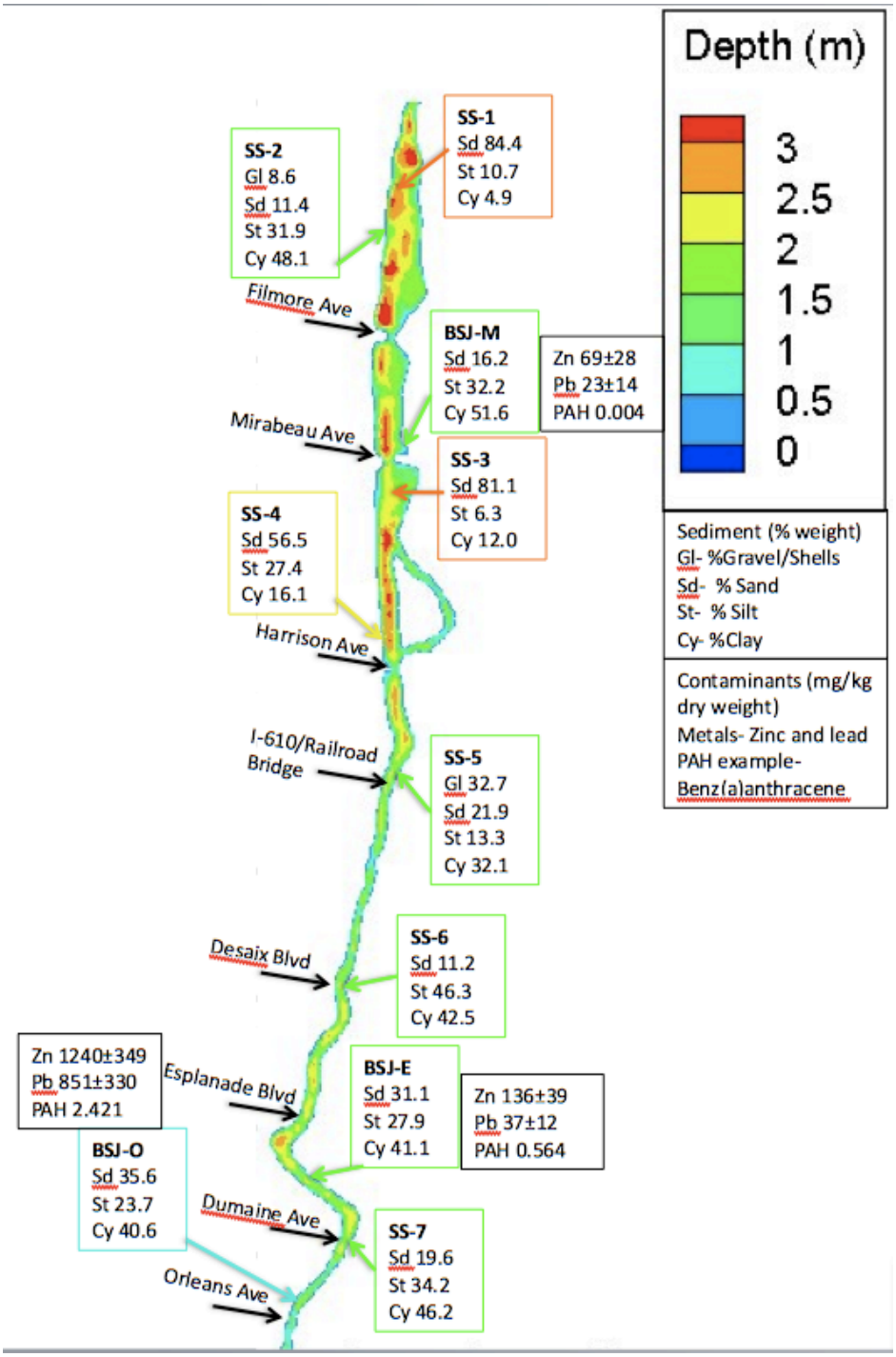

Figure 4. Representation of bathymetry in Bayou St. John (Martinez et al., 2008) as it relates to grain size in the bottom sediment. The SS-x samples were collected during this study and the BSJ-x samples were collected and analyzed by Mowat and Bundy (2001). The color of the outline surrounding each sediment sample and arrow links the sample to the approximate location and depth the sample was collected from. The black boxes are examples of contamination recorded at each BSJ-x location (Mowat and Bundy, 2001). The black arrows delineate the location of bridges crossing Bayou St. John.

Table 4. Representative sample of sediment contamination levels in Bayou St. John from South to North taken from Mowat and Bundy (2001) compared to Canadian federal guidelines.

Metals in mg/kg dry wt.	Cadmium	Chromium	Copper	Lead	Nickel	Zinc
Orleans	ND	30.8	143	1140	28.7	105
Dumaine	7.87	15.1	208	851	32.9	1240
Esplanade	ND	39.9	115	36.5	30.2	136
Mirabeau	ND	43.8	17.9	22.6	18.5	69.2
Lower Limit	*0.6*	*26*	*16*	*37*	*16*	*120*
Impaired	*10*	*110*	*110*	*250*	*75*	*820*
Freshwater Guideline	*0.6*	*37.3*	*35.7*	*35*		*123*
Limit for Probable Effect	*3.5*	*90*	*197*	*91.3*		*315*

PAH in mg/kg dry wt.	Naphthalene	2-Methyl naphthalene	Phenanthrene	Benz(a)anthracene	Pyrene
Orleans	0.195	0.251	8.091	4.07	29.31
Dumaine	0.51	0.255	3.545	2.421	18.79
Esplanade	0.026	0.016	0.104	0.564	2.51
Mirabeau	0.007	0.004	0.007	0.004	0.052
Freshwater Guideline	*0.035*	*0.02*	*0.042*	*0.032*	*0.053*
Limit for Probable Effect	*0.391*	*0.201*	*0.315*	*0.385*	*0.875*

Yellow highlights indicate levels above Freshwater guidelines and Red highlights indicate levels above impaired or probable effect criteria.

Water Elevation

The field data captures two cold fronts and therefore by design shows large changes in water surface elevation. Figure 5 shows the change in water surface elevation captured at each location during field-testing. The field data collected during this study shows the water elevation in Bayou St. John never rises above the water elevation of Lake Pontchartrain and only occasionally equals the water elevation in the restricted zone. The trends in water surface elevation change are mirrored across the waterfall structure; however there are several time segments when the Bayou water surface elevation rises higher or drops lower than the inlet water surface elevation. These discrepancies are most likely due to anthropogenic withdrawal and precipitation input. Bayou St. John has a much larger surface area than the restricted zone and therefore will receive more direct precipitation. As discussed above, levees prevent the restricted zone from receiving run-off, but Bayou St. John acts as a drainage basin for surrounding neighborhoods. In addition, when the surface water elevations in Bayou St. John reach a peak, the local Sewerage and Water Board operators open a valve at the southern end of Bayou St. John to prevent localized flooding around the Bayou causing the water elevation to drop faster and to a greater degree than the inlet. The large impact anthropogenic discharge from Bayou St. John has on the observed field water

elevations indicates the north Bayou observed values are a result of discharge and cannot be used to force hydrodynamic modeling.

The water elevation in Bayou St. John shows a downward trend while the water elevation in Lake Pontchartrain recovers to water elevation around 0.3 m as each subsequent cold front occurs. Water fluctuations captured by Schindler (2009) show a much different picture, where the Bayou water elevation are maintained at a relative high while water elevations in Lake Pontchartrain dropped steeply. This flow reversal depicts normal inlet behavior during a storm. The disparity in the two data sets is evidence and may be attributed to a (1) the fact that the Schindler (2009) dataset did not obtain survey data to unify the water surface elevations between the Bayou and the Lake, and hence the flow reversal may not be present at all, or (2) it demonstrates that a continuous discharge withdrawing water from Bayou St. John was present during this study, most likely at one of the S&W Board controlled valves. The selected period for field deployments is known for the presence of frontal weather accompanied by large fluctuations in water level driven by Lake Pontchartrain.

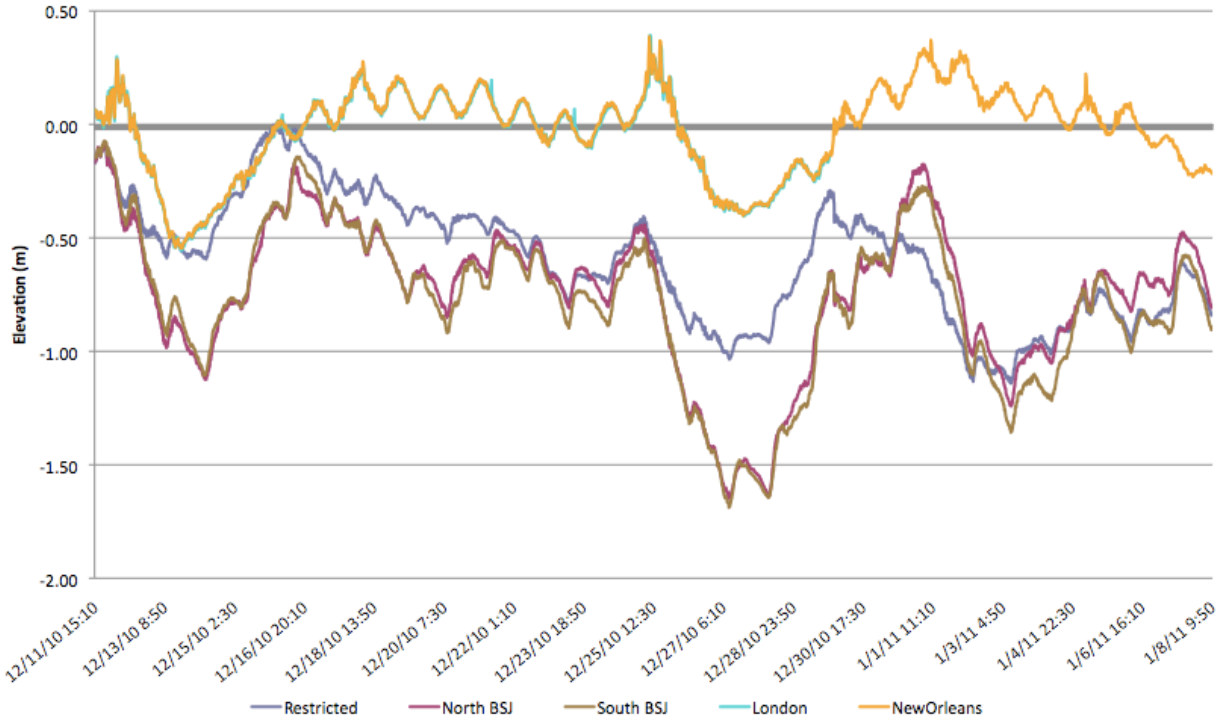

Figure 5. Time dependent water surface elevation in meters (relative to NAVD 88 m) in Bayou St. John compared to those of Lake Pontchartrain (denoted by the two outfall canals), the restricted zone, and north and south Bayou St. John as observed during field data collection.

Since all field data was collected at the same time period were converted to the same datum, energy loss between the relative locations can be directly calculated. Figure 5 depicts the

instantaneous water elevation, the difference of which is defined as total energy losses between the three zones: Lake Pontchartrain, inlet or restricted zone, north Bayou St. John, and south Bayou St. John. Positive energy loss indicates restriction to flow as water travels south into the Bayou while a negative energy loss indicates flow reversal towards the north. The average energy loss from Lake Pontchartrain through the sector gates into the restricted zone is 0.56m (range 1.36 to – 0.09m). This large amount of energy loss is partially due to the sector gates and partially due to a sand bar located at the mouth of the inlet. The average energy loss from the restricted zone through the waterfall structure is 0.16 m (range 0.68 to -0.40 m). This data does not give an equal representation of forward and reverse flows due to an unknown discharge from within Bayou St. John, however the energy loss is approximately half the energy loss observed from Lake Pontchartrain through the sector gates. This illustrates that the sector gates are the primary source of energy dissipation, although the waterfall structure contributes to additional energy loss, and provides a significant blockage to tidal induced mixing. Water openly flows from north to south within Bayou St. John as is shown by equivalent maximum forward and reverse energy loss of 0.20m and -0.18m between the north and south water elevations.

Water velocities recorded by the Aquadop meter show the maximum flow through the culverts was 0.05 m/s in either direction during field observations. Flow during field observations vacillated between flow in and out with a magnitude of approximately 24 hours.

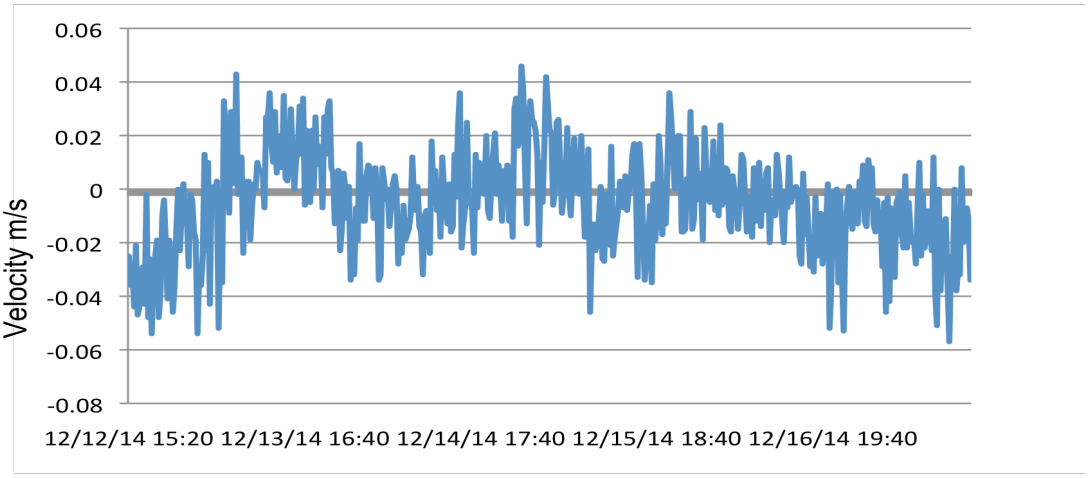

Figure 6. Water velocities recorded at the north end of Bayou St. John indicative of forward and reverse flow through the waterfall structure.

Analysis of Water Parameter Variability

Table 5 shows the range and average temperature, salinity, conductivity, and turbidity recorded during field data collection. Turbidity showed more variability than the other measured parameters. During high winds and rapid increases in water elevation during cold fronts, the

turbidity increases indicating suspension of solids in the water column. The spikes in turbidity are stronger at the north end of Bayou St. John than at the south end. Increased turbidity at the north end is most likely linked to sediment being transported into the Bayou from the restricted zone, which maintained a relatively high turbidity throughout filed data collection. Most of the turbidity seen in spikes at the southern end of Bayou St. John and a portion of the turbidity recorded at the north end is also likely due to sediment resuspension during the higher wind and currents from the corresponding cold front. Schindler (2009) showed a similar response in turbidity with sudden spikes appearing in the data that correlated to the onset of cold fronts.

Table 5. Field Data Summary for Bayou St. John (2010-2011)

	Temperature C	Sp. Conductivity	Salinity ppt	TDS g/L	Turbidity NTU
Restricted Zone Bayou St. John December 13, 2010 to January 8, 2011					
Maximum	16.35	5.52	3.00	3.59	16.60
Minimum	5.93	5.17	2.80	3.36	16.20
Average	10.84	5.34	2.90	3.47	16.40
North Bayou St. John December 13, 2010 to January 8, 2011					
Maximum	15.77	5.44	2.94	3.54	23.00
Minimum	7.60	5.12	2.76	3.32	0.00
Average	11.66	5.31	2.89	3.45	0.00
South Bayou St. John December 13, 2010 to January 8, 2011					
Maximum	16.24	5.82	3.17	3.79	13.30
Minimum	7.77	5.31	2.88	3.45	0.00
Average	11.58	5.50	2.99	3.58	0.00

Temperature and salinity had very subtle changes from north to south. The southern end of the Bayou had a change of less than 1°C and 0.2 ppt from the north end of the Bayou during time of deployment. Despite these subtle changes, the trends of temperature and salinity closely follow environmental conditions. Figure 7 shows the water temperature and salinity response to cold fronts during the field data collection. The data shows that water temperature decreases rapidly with the onset of a cold front in response to the drop in air temperature. Both the restricted zone and Bayou St. John are shallow water bodies with a relatively small heat capacity. The field data shows the restricted zone loses heat more rapidly than Bayou St. John most likely due to an influx of cooler Lake Pontchartrain water while the Bayou remains more susceptible to heat flux from the atmosphere. Salinities in the restricted zone and north Bayou St. John are similar, which is reasonable based on the close proximity of the two stations. The salinity in the southern region of Bayou St. John begins the sampling time period with a relatively elevated salinity (3.77 ppt) that slowly decreases to a value similar to that in the northern end (2.88 ppt). This is further evidence of longitudinal mixing caused by either wind-stress or flow induced mixing produced by flow

withdrawal; this would draw water from the north to the south flushing the lower segment with less saline water.

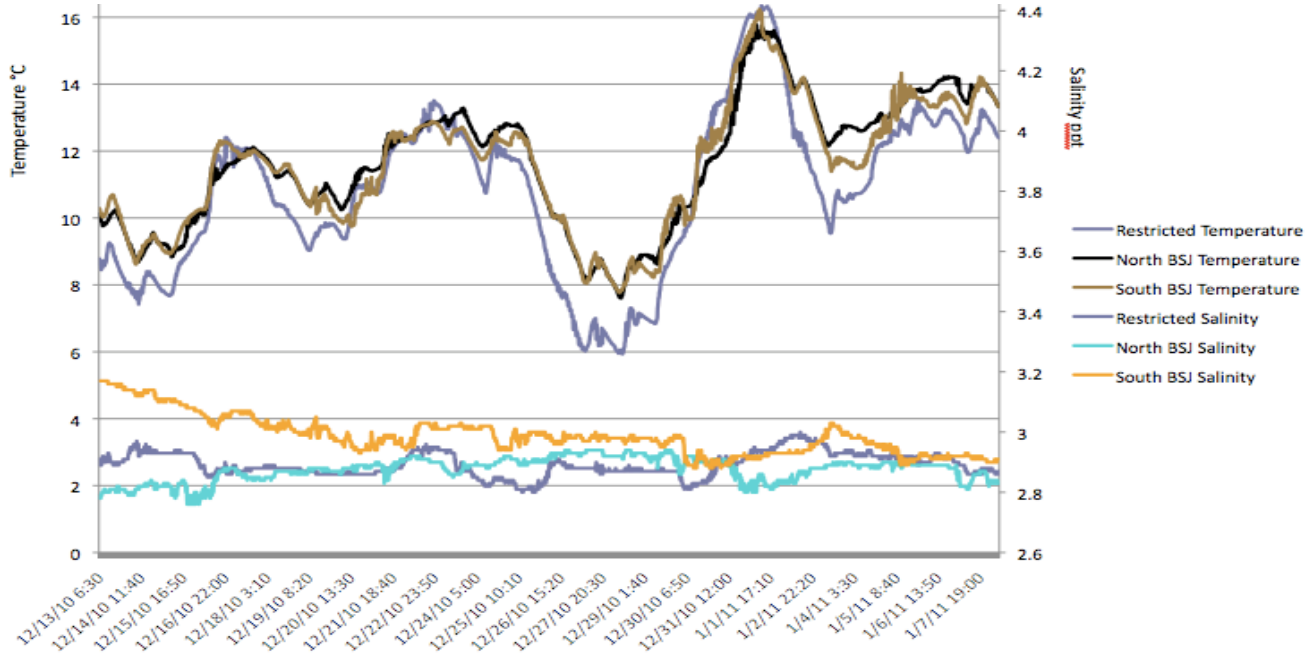

Figure 7. Temperature and salinity recorded within Bayou St. John during December 2010 and January 2011 field data collection.

Results and Implementation of 1-D Model

The model was calibrated using field data at z_2 and z_4 by adjusting unknown values at the waterfall culverts, which include the K_L value, manning's n through the culverts, and the actual diameter of the culverts. The K_L value was set at a conservative estimate of 7 based on the butterfly valves being open at a 45° angle. A range of values for K_L from 0.1 to 150 was then used to calibrate the fit of the results to field data. Mannings n was tested from a range of 0.022 for culverts and 0.029 for rubble. The diameter of the culverts was tested from a range of 3 m for unimpeded flow and 0.5 m as assumed in the BKI (2000) model.

Field water elevations from z2 and z4 were used to analyze field velocity characteristics through the waterfall culverts. Field water surface elevation head loss plotted against velocities calculated using field display a slope of 0.2264x+0.1576 with an r^2 value of 0.9669. This slope is used to replace the culvert velocity equation in the final model. After calibration, the constants for the 1-D equations were determined as follows:

$$A_2 = b_2 y_2$$
$$P_2 = 2b_2 + 2y_2 \quad ; \text{b=26.21m} \qquad \textbf{(19)}$$

$$V_2 = \left(\frac{1}{0.025}\right)0.01414\left(R_2^{2/3}\right)$$; S_0=0.0002, n=0.025 **(20)**

$A_3=y_2(38.5 + 1.75y_2)$; b=38.5m, z=1.75 (side slope of channel) **(21)**

$$z_3 = \frac{V_3^2}{2g} - z_2 - \frac{V_3^2}{2g} - K_e$$;K_e = head loss from expansion **(22)**

$V_p=0.2264(z_3-z_4) +0.1576$; area of culverts is 3.53 m^2 **(23)**

$$z_4 = -(H_L - z_3 + L_P\left(\frac{n}{D^{5/3}}\right)^2$$

$$H_L = 0.5\frac{V_3^2}{2g} + \frac{V_3^2}{2g} + K_L\frac{V_3^2}{2g}$$; H_L= head loss term, n=0.029 **(24)**

Figure 8 shows the predicted water elevation of the 1-D model compared to observed water elevations on either side of the waterfall structure. The three variables were tested incrementally to understand each variables impact on the resulting water elevation. At a Manning's n of 0.0029 the culvert friction term had little impact on resulting water elevations. The most significant variable in terms of predicted water elevation was the K_L term. Use of this model resulted in linear loss of energy between the inlet and north Bayou, which cannot account for the changes in water elevation observed across the waterfall structure. This indicates the increased magnitude of the north Bayou signal is due to factors other than friction such as turbulence and drag in the culverts due to accumulated, meteorological impacts, and manual operation of the sluice gates.

Figure 8 shows the 1-D model predicted water elevations compared to the observed field data. Table 6 shows the analysis of the 1-D predicted north Bayou water elevations compared to the north Bayou observed water elevations using statistical analysis. The analysis shows the predicted values are within approximately 75% of the observed and the tidal signal is recovered shown by an index of agreement of 95%. The above equations uniformly lower the water elevation but do not capture the north Bayou water elevations close enough to warrant using this data to complete 3-D simulations. Observed field data will be used in place of the 1-D predictions and simulation 2 described in Table 2 will not used.

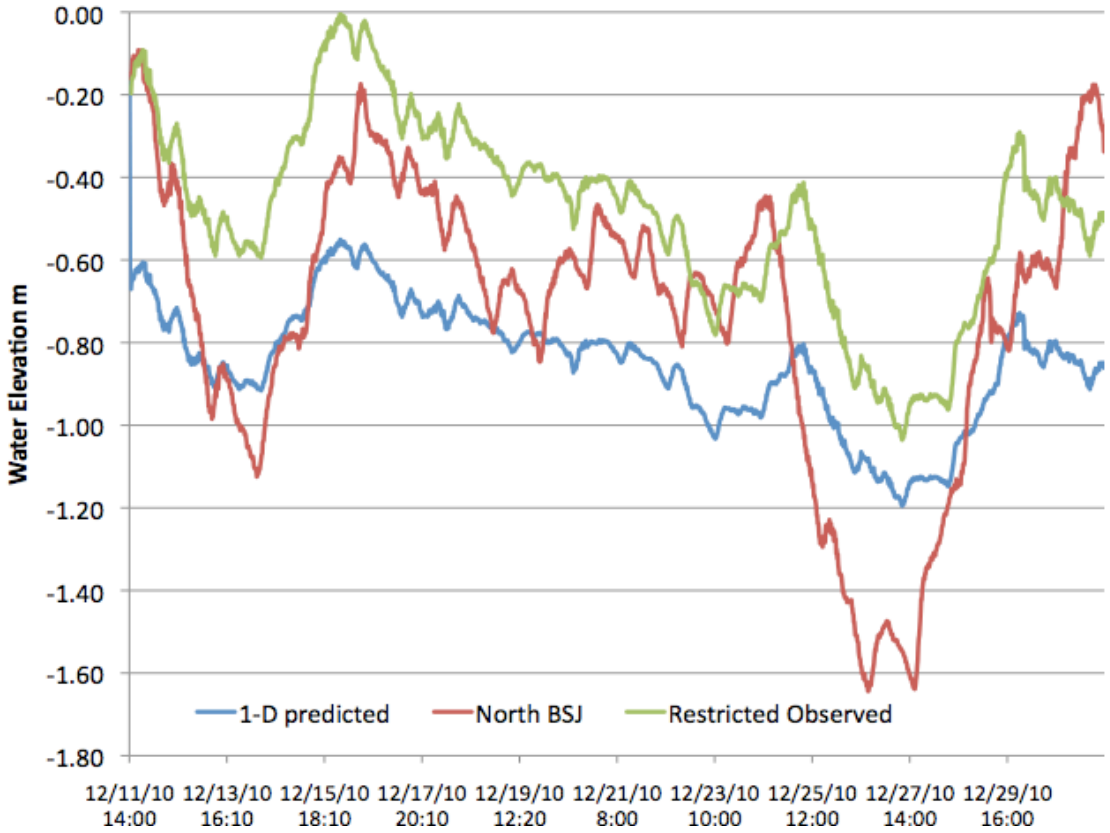

Figure 8. Results of predicted water surface elevation in Bayou St. John based on the 1-D equations shown in comparison to field observations during field deployment. A K_L value of 130 was used for this simulation.

Table 6. Statistical analysis of 1-D predicted water surface elevations in North Bayou St. John compared to observed values.

1-D Model	Correlation	RME	RMSE	d
North BSJ	0.67	0.25	0.29	0.93

ECOMSED Model Calibration

The model calibration predicted the observed water elevations in south Bayou St. John very closely with a 95% correlation, 97% signal match, and average deviation of 0.07 m (Table 7). Water elevations predicted by the model at the north and south locations have a 100% correlation between them. This contrasts the observed data, which shows a phase lag and separation between the north and south water elevations. Figure 9 shows the predicted water elevation at the south location compared to observed field data within the Bayou and in the restricted zone. The predicted water elevations to the north end of the Bayou also have a 95% correlation but the average deviation is slightly higher at 0.06 m. The predictions lag slightly behind the north observed water elevation signal because the north observed water elevations were moved

upstream near the open boundary for calibration. This lag is revealed in the statistical analysis though the signals are identical. The south observed water elevations show peaks and valleys above and below the north observed water elevations. These differences are not captured by the calibration, which indicates the meteorological forcing at 10%, notably evaporation and precipitation, in addition to anthropogenic withdrawal, are insufficient to completely account for the water volumes added and removed from the southern end of the Bayou.

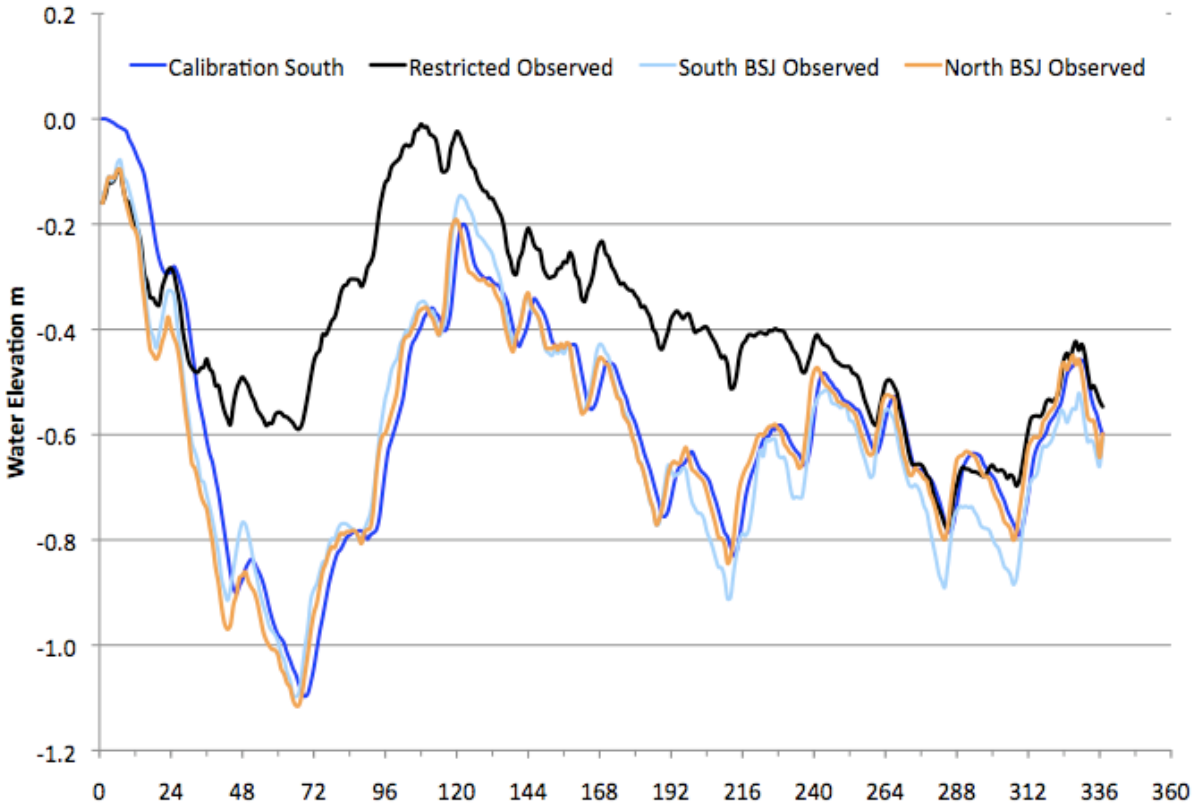

Figure 9. Comparison of the predicted water surface elevations of the calibrated model at 10% meteorological forcing to the observed water surface elevations at the north and south end of Bayou St. John.

Sensitivity Testing

Time-dependent meteorological boundary conditions and bottom roughness were modified to test the sensitivity of the calibrated model. Meteorological values can impact the water mass balance of the Bayou through evaporation and precipitation, mixing and water velocities through wind impact, and temperature and salinity through heat flux, evaporation, and precipitation. These impacts were anticipated to have an exaggerated effect in the Bayou because the Bayou is both shallow and narrow. Meteorological forcing was uniformly increased, both spatially and as a time-dependent variable, to 25% of open water conditions and uniformly decreased to 0% open water conditions in two different sensitivity tests. Bottom roughness can impact shear stress by altering

bottom velocities and retard flows through increased friction. The bottom roughness was uniformly increased at all nodes to 0.003 during the sensitivity test.

The model robustly predicted water elevations close in statistical value to the observed water elevations during all sensitivity tests (Table 7). Water elevations showed 100% correlation between the sensitivity models. This indicates increasing roughness to 0.003 and increasing meteorological forcing to 25% cannot account for the difference between the north and south observed water elevations.

Table 7. Statistical analysis of ECOMSED predicted water surface elevations in Bayou St. John compared to observed values.

North BSJ	**Correlation**	**RME**	**RMSE**	**d**
Base Calibration 10% Meteorological Force	0.95	0.05	0.07	0.97
0% Meteorological Sensitivity Test	0.95	0.05	0.07	0.97
25% Meteorological Sensitivity Test	0.95	0.05	0.07	0.97
Roughness Sensitivity Test, 0.003	0.95	0.05	0.07	0.97
South BSJ	**Correlation**	**RME**	**RMSE**	**d**
Base Calibration 10% Meteorological Force	0.95	0.06	0.08	0.97
0% Meteorological Sensitivity Test	0.95	0.06	0.08	0.97
25% Meteorological Sensitivity Test	0.95	0.07	0.08	0.97
Roughness Sensitivity Test, 0.003	0.95	0.06	0.08	0.97

Model Validation

Water temperature and salinity are transported in a similar manner in ECOMSED; however, transport is balanced by impact from meteorological forcing. Figures 10 and 11 show the time-dependent predicted temperature and salinity values for the base calibration and meteorological forcing sensitivity tests compared to observed field values. The roughness sensitivity test predicted values close to the base calibration and 0% meteorological forcing simulations. Table 8 shows the statistical fit of observed and predicted values for all calibration and sensitivity simulations. All three simulations show very little correlation to observed salinities or temperature. The correlations were approximately 79% of the observed values for the base calibration, 0% meteorological forcing, and roughness test indicating the general trends were similar, but the values of individual points did not overlap. Salinity statistical alignment increased as meteorological forcing was decreased but temperature statistical alignment increased with increasing meteorological forcing. This is caused by the fact that both predicted variables decrease early in the model similar to observed temperatures, while observed values of salinity were relatively stable. The predicted temperatures mimic the response of the observed values throughout the simulation but at an attenuated magnitude and salinities show a time-dependent response similar to temperature that is not present in the observed values. This indicates that one or more components of the meteorological forcing are out of phase or have different actual

magnitudes when compared to observed conditions. Moreover, since meteorology was obtained from open water conditions 3 km away from the Bayou, it's possible that the actual local values are not the same. Observed values for temperature are on average 4°C warmer than predicted values and salinities are approximately 0.9 ppt higher than predicted values for the base calibration. Statistical parameters from the calibration and all sensitivity tests as can be seen in Table 8. The index of agreement for temperature and salinity are between 16% and 45% based on the amount of delay before a response was observed. This equilibration period appears to affect the model skill assessment although it is misleading. In other words, once the absolute values equilibrate, the model does capture the variability observed in the field.

An inverse relationship can be seen between increased and decreased meteorological forcing between the north and south locations where temperatures are cooler and salinities decrease with increasing meteorological forcing in the north but the temperature and salinity are higher with increased meteorological forcing in the south. As the cold front descends, both air and water temperature quickly drop in Lake Pontchartrain and the increased precipitation lowers salinities. Both of these impacts can be observed in the model with cooler, less saline water entering Bayou St. John from the north causing salinities to decrease from the initial condition of 3 ppt to approximately 2.7 ppt. At 72 hours the predicted salinities and temperature rapidly decrease then stabilize at much lower values for the remainder of the simulation. Water elevations at 72 hours were at the lowest elevation at -1.1 m leaving less than one meter of water along the banks of the Bayou. With a high surface area and low water column height, the north Bayou was most susceptible to meteorological forcing at this time period. This event is also at the height of the cold front when air temperatures are low, wind is high, and precipitation is high. Cold rain will both depress water temperature and salinities, heat flux would be towards the atmosphere, and the wind would increase mixing allowing the meteorological forcing to impact the full water column. The south location of the Bayou also experienced low water elevations to -1.1 m, however this section of the Bayou remains shallow and is much more narrow than the north limiting the amount of precipitation the south end receives. The low fetch and Bayou sinuosity also limits the impact wind can have on the water column. The data also indicates the south does not respond to transport of temperature and salinity until much later in the simulation indicating the water column did not receive lower salinity and cooler water during the time period when water elevations were low. Despite small anticipated differences, wind forcing and heat flux are expected to be similar from north to south indicating the most important variable that causes a discrepancy between the locations is direct precipitation due to surface area differences from north to south.

Precipitation may also be responsible for the rapid loss of salinity at the south location within the first few hours of simulation. Reducing precipitation uniformly across the Bayou in excess of other meteorological parameters may increase the salinity and temperatures of both the north and south locations.

Table 8. Statistical analysis of ECOMSED predicted temperature and salinity in Bayou St. John compared to observed values.

	Salinity				**Temperature**			
North BSJ	**Correlation**	**RME**	**RMSE**	**d**	**Correlation**	**RME**	**RMSE**	**d**
Base Calibration	0.78	0.83	0.91	0.45	0.20	3.90	4.29	0.24
0% Meteorological Sensitivity Test	0.80	0.82	0.90	0.46	0.21	3.87	4.29	0.23
25% Meteorological Sensitivity Test	0.73	0.87	0.96	0.44	0.12	4.17	4.54	0.25
Roughness Sensitivity, 0.003	0.80	0.82	0.90	0.46	0.22	3.88	4.29	0.23
South BSJ	**Correlation**	**RME**	**RMSE**	**d**	**Correlation**	**RME**	**RMSE**	**d**
Base Calibration	0.31	0.35	0.37	0.24	0.59	1.40	1.73	0.25
0% Meteorological Sensitivity Test	0.40	0.37	0.40	0.24	0.67	1.50	1.82	0.16
25% Meteorological Sensitivity Test	0.03	0.31	0.34	0.23	0.60	1.42	1.79	0.37
Roughness Sensitivity, 0.003	0.27	0.35	0.38	0.24	0.68	1.44	1.76	0.21

In all simulations the south predicted temperature and salinity lagged in response time compared to the north predicted temperature and salinity, indicating flow from north to south continually adjusts equilibrium with climatic factors (Figures 10 and 11). Temperature changes based on sensitivity tests show that increased meteorological forcing depresses the temperature in the north and delays the Bayou response to temperature in the south by 120 simulated hours more than the base calibration or other sensitivity tests, which have a delay of 72 simulated hours. Both temperature and salinity have the same delay times indicating the delayed response is due to transport mechanisms from north to south. The south responds to tidal fluctuations forced at the northern open boundary within a few hours once the response has been excited, however the tidal signal is attenuated and the changes are smooth compared to the sharp fluctuations in predictions at the north end of the Bayou.

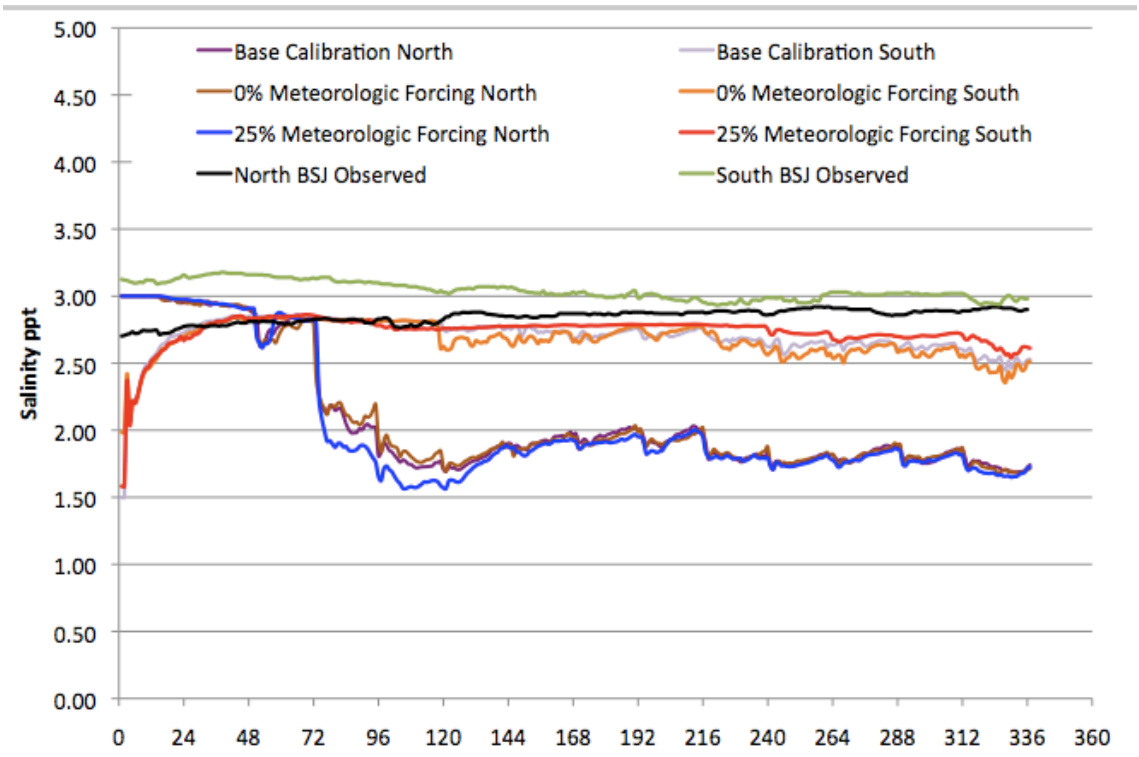

Figure 10. Predicted time-dependent salinity at the north and south locations within Bayou St. John for the base calibration compared to each sensitivity test and the observed values.

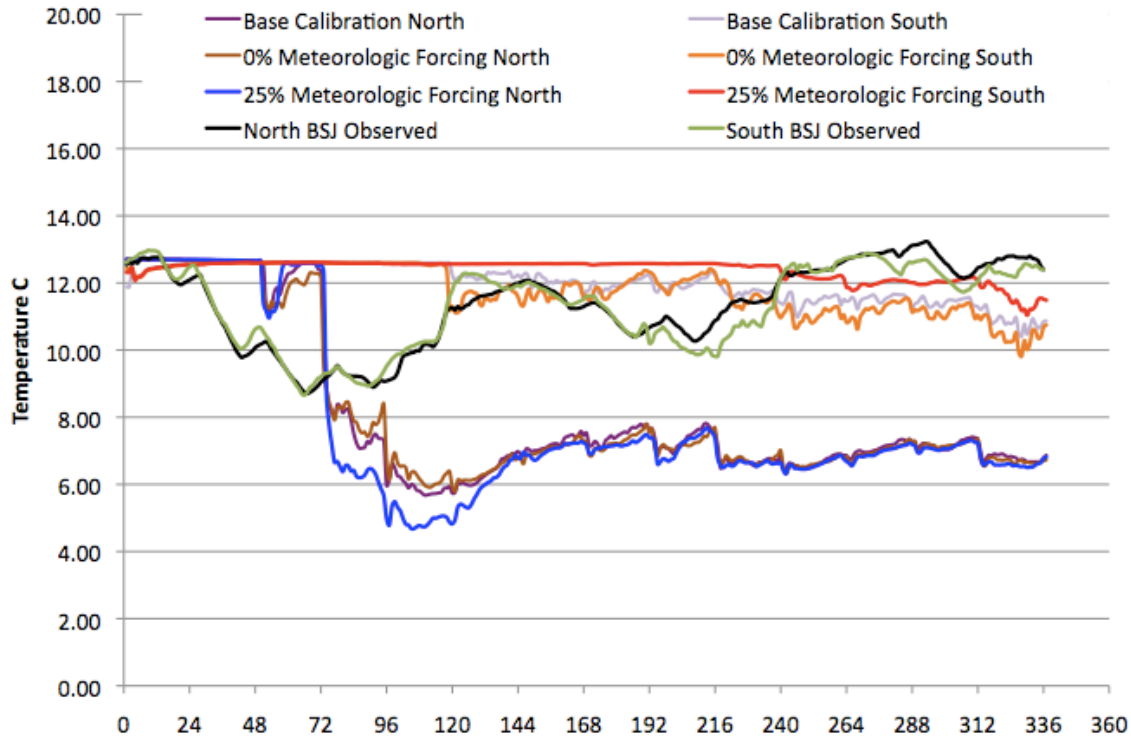

Figure 11. Predicted time-dependent temperature at the north and south locations within Bayou St. John for the base calibration compared to each sensitivity test and observed values.

Hydrologic Characteristics

Mixing and Tidal Exchange Flow

The general hydrologic characteristics of Bayou St. John can be described with an analysis of mixing and tidal exchange along the Bayou. Table 9 shows the bulk Richardson numbers. A large bulk Richardson number is indicative of stratification while low numbers indicate a well-mixed system. The Bayou has limited flow, which causes large mathematical differences in the bulk Richardson number. The low energy of the system results in unrealistically elevated bulk Richardson numbers and prevents a direct analysis of the values, however the relative differences between the simulations can be analyzed.

Low predicted velocities from north to south in the Bayou result in very large bulk Richardson numbers despite that the water has reasonably low changes in density from surface to bottom or low buoyancy from surface to bottom conditions. Changes in density follow the same pattern as velocity where higher gradients exist in the north due to increased depth than exist further south. The middle of the Bayou has similar depth and velocities as the north. At simulation time of 40 and 80 hours the water surface elevation is rapidly dropping and rising respectively in response to a cold front and therefore represents time periods of high flow. After 180 hours of simulation the water elevations are stable representing a time period of moderate flow through the Bayou. Bulk Richardson numbers reflect this difference for simulation hours 80 where the values are higher than at simulation hour 180. At a simulation time of 40 hrs water elevations are decreasing from the resting initial condition as the model equilibrates in addition to decreasing in response to the first cold front signal. The resulting velocities are higher than at any other time in the simulation. The slight increase in velocities during this time period at the beginning of the simulations decrease the bulk Richardson number revealing the sensitivity this equation has to small changes in velocity.

Velocities have to be above 0.02 m/s and the density gradient must be below 0.008 kg/m^3 for mixing to occur in Bayou St. John. A bulk Richardson number above 0.8 indicates stratification. Stratification becomes more prevalent with distance from the open boundary in the north due to both an increased density gradient and decreased velocities. Bulk Richardson numbers are elevated more due to decreasing velocities than to density gradients with increasing distance south. Figure 12 shows the time dependent bulk Richardson numbers as daily averages for the base calibration and each sensitivity test and Figure 13 shows increasing bulk Richardson numbers with increased distance to the south. The bulk Richardson numbers show a similar pattern as was observed for temperature and salinity where decreased stratification occurs at 72 hours in the

simulation. At the lowest water elevation water velocities are higher and the low water column height allows wind to have a larger impact on mixing. As the water elevation rapidly rises after the cold front passes, the opposite effect occurs where the water column height increases and wind impact is felt only on the surface water (wind straining), which can increase gradients from surface to bottom. As the water elevation, and water column height, slowly decreases through the simulation period the meteorological forcing is again able to decrease stratification. The opposite effect is seen in the 0% meteorological forcing sensitivity test where density gradients are a component of transport only and velocities are high when water elevations change rapidly, leading to lower bulk Richardson numbers, and velocities are low later in the simulation period when water elevation changes are more gradual, leading to higher bulk Richardson numbers. The majority of the calibration falls between the two sensitivity tests. This suggests that meteorological forcing can have a large impact on mixing in Bayou St. John.

Table 9. Statistical analysis of vertical mixing in Bayou St. John for the calibration and sensitivity simulations using bulk Richardson number (Ri_L) relative to velocity (U) and density gradient ($\Delta\rho$) from surface to bottom. Values were averaged across transects at the North and Mid locations and sampled as a discrete value at the South location. Values were derived after a simulation time of 40, 80, and 180 hours.[1]

Simulation Name	Sim. Hour	**Ri_L**			**U**			**$\Delta\rho$**		
		North	Mid	South	North	Mid	South	North	Mid	South
Base Calibration	40	2.99	3.92	25.7	0.021	0.019	0.006	0.083	0.054	0.018
	80	70.6	88.9	399	0.006	0.006	0.002	0.170	0.112	0.022
	180	2.06	1.11	10.5	0.010	0.012	0.003	0.011	0.006	0.002
0% Meteorological Sensitivity Test	40	2.02	3.62	21.9	0.022	0.021	0.008	0.060	0.056	0.029
	80	62.2	49.7	90.5	0.006	0.005	0.002	0.126	0.125	0.012
	180	0.363	0.911	18.3	0.009	0.010	0.004	0.002	0.003	0.007
25% Meteorological Sensitivity Test	40	0.273	2.71	15.5	0.021	0.020	0.010	0.008	0.040	0.010
	80	31.6	22.7	1021	0.006	0.006	0.001	0.083	0.029	0.039
	180	1.32	1.86	18.1	0.010	0.010	0.004	0.007	0.006	0.005
Roughness Test, 0.003	40	2.00	3.59	12.1	0.021	0.020	0.006	0.060	0.056	0.019
	80	65.3	55.3	121	0.005	0.005	0.002	0.128	0.121	0.016
	180	0.35	0.84	13.4	0.010	0.010	0.003	0.002	0.003	0.006

Table 10 shows the flow, velocity, and bottom velocities for each simulation. Flows were calculated using the along Bayou component of velocity (north component –V). Despite rapid equalization of water elevations through the Bayou, instantaneous snapshots of flow show substantial energy loss from north to south within the Bayou. More than half the energy present at the north end of Bayou St. John is dissipated en route to the south at all flow volumes. This loss in

[1] Yellow highlighted values are mixing while orange numbers indicate values that are between fully mixed and fully stratified.

energy is associated with the many restrictions and changes in flow direction dictated by the complex geometry within the Bayou. Additional restrictions are present at the south location from the sinusoidal bank geometry reminiscent of the Bayou's historical origin as a stream connection between the Mississippi River and Lake Pontchartrain. The loss in flow diminishes bottom velocities from north to the midpoint. Figure 14 shows time dependent flow for the base calibration and sensitivity tests as a moving daily average. Increasing meteorological forcing also increased the flow denudation in the south location for the majority of the simulation period. At simulation hour 192 to opposite was true where meteorological forcing increased flow, likely due to a change in wind direction. Increased bed roughness increased the internal friction of the Bayou and depressed tidal exchange flow from north to south.

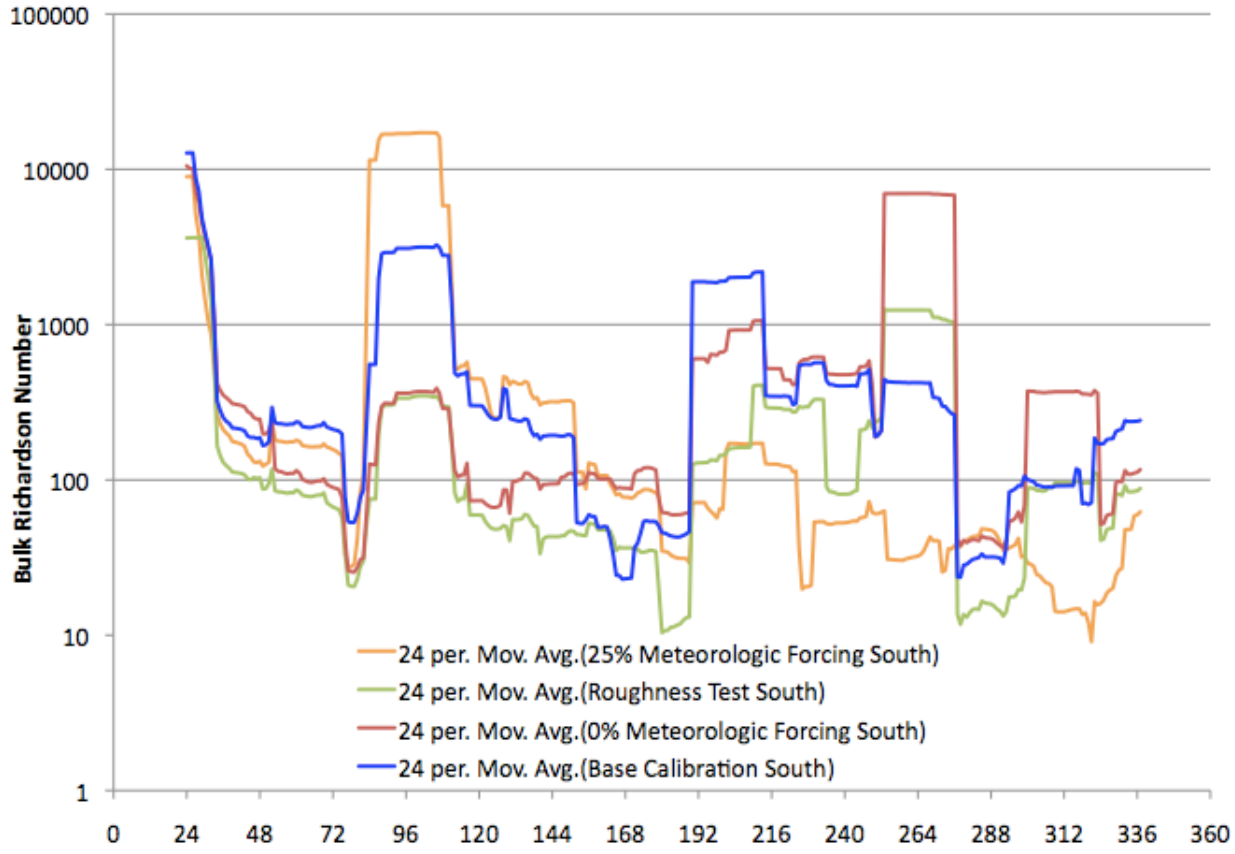

Figure 12. Bulk Richardson number comparison between the base calibration and sensitivity testing. Values are expressed as time-dependent, daily averages.

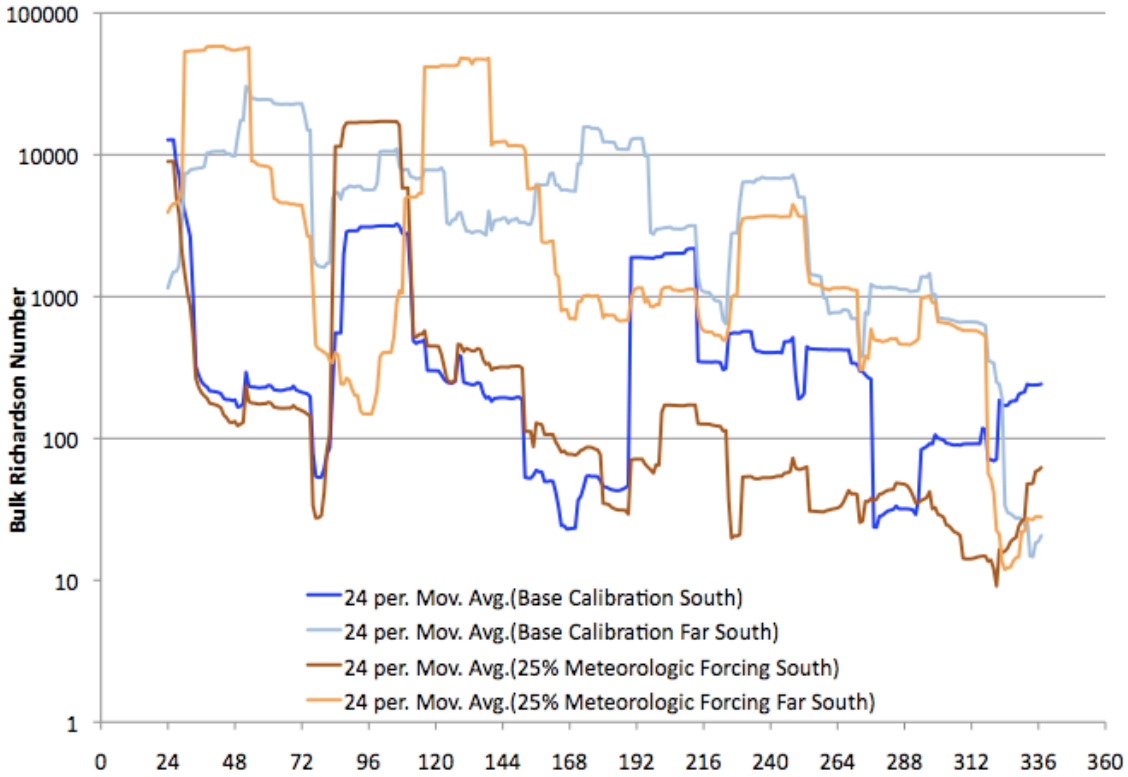

Figure 13. Bulk Richardson number comparison between the base calibration and 25% Meteorological Forcing sensitivity test between the south and far south locations.

Table 10. Analysis of Flow, Average bottom velocity, and maximum bottom velocity predicted across transects at the north and mid and as discrete samples at the south location within Bayou St. John for each calibration and sensitivity analysis for instantaneous times at simulation hour 40, 80, and 180.

Simulation Name	Sim. Hours	**Q m^3/s**			**Ub_{ave} m/s**			**Max Ub m/s**	
		North	Mid	South	North	Mid	South	North	Mid
Base Calibration	40	-4.75	-5.16	-0.542	0.005	0.003	0.007	0.006	0.004
	80	1.31	1.33	0.138	0.009	0.008	0.003	0.012	0.014
	180	-2.39	-2.02	-0.296	0.008	0.003	0.001	0.010	0.004
0% Meteorological Sensitivity Test	40	-4.99	-5.79	-0.744	0.007	0.003	0.004	0.009	0.005
	80	1.21	1.56	0.212	0.013	0.005	0.002	0.017	0.007
	180	-2.47	-2.77	-0.413	0.008	0.005	0.001	0.010	0.007
25% Meteorological Sensitivity Test	40	-4.80	-5.95	-0.608	0.013	0.008	0.008	0.016	0.011
	80	1.35	1.33	0.120	0.006	0.017	0.001	0.012	0.020
	180	-2.55	-3.25	-0.346	0.009	0.004	0.002	0.011	0.005
Roughness Test, 0.003	40	-5.21	-5.63	-0.231	0.006	0.003	0.008	0.008	0.004
	80	1.21	1.46	0.057	0.012	0.005	0.003	0.015	0.007
	180	-2.59	-2.87	-0.132	0.009	0.005	0.001	0.011	0.006

Shear Stress Analysis

Figure 15 shows the time dependent applied shear stress values for the base calibration and sensitivity tests. None of the extracted locations exceeded the critical shear stress value of 0.1 N/m^2 (Haralampides, 2000). As shown with tidal exchange flow, the 0% meteorological forcing sensitivity test had the highest shear stress numbers with a maximum shear stress of 0.018 N/m^2 at the north end of the Bayou. Energy dissipation from north to south causes shear stress values to also decrease from north to south. No resuspension is predicted within in the Bayou and transportation is limited to the north and middle of the Bayou.

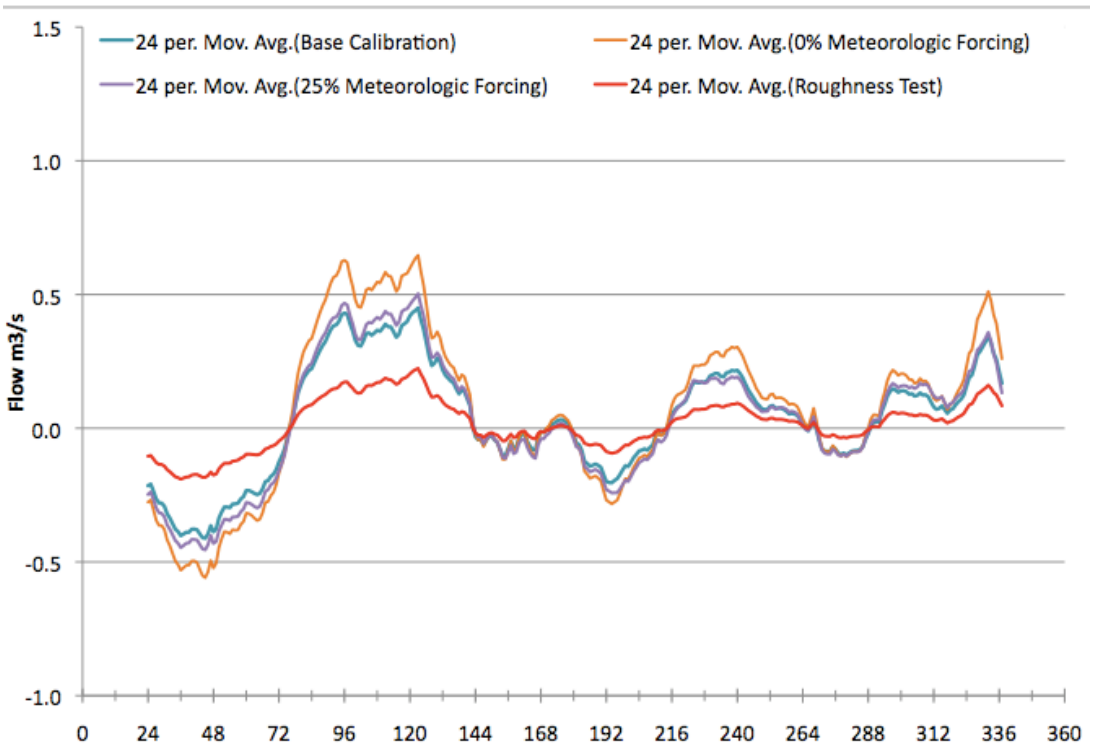

Figure 14. Comparison of time-dependent flow for the base calibration and all sensitivity tests. Flows are shown as daily averages through the simulation period. Positive flow is into the Bayou (toward the south) and negative flow is to the north.

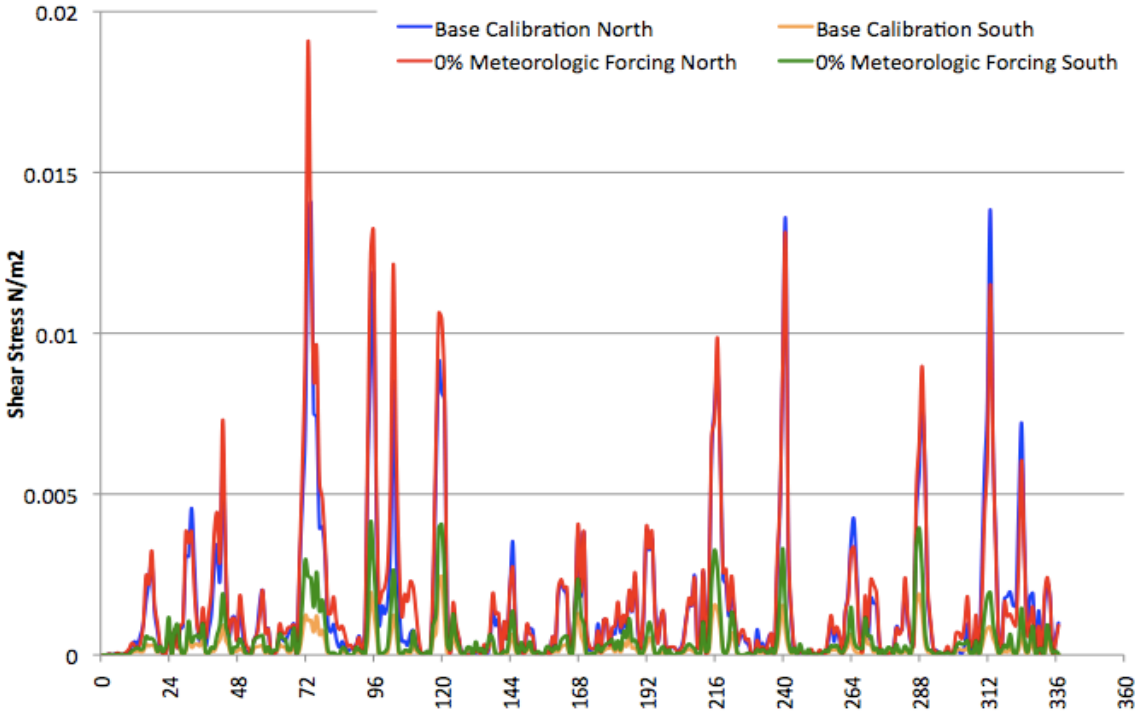

Figure 15. Shear stress analysis for the base calibration compared to sensitivity tests for both north and south locations.

Analysis of Simulations

Surface Water Elevation Simulation Results

The calibration simulation was used as a reference for all additional simulations, referred to as the calibration model from this point forward. Simulations were used to test the different hydrologic characteristics of tidal forcing with the waterfall structure, once the waterfall structure was removed, and with both the waterfall structure removed and sector gates fully open. Direct field measured water elevations can be used to test these simulations because the observed water elevations at the north section of Bayou St. John represent energy losses through the waterfall structure and observed water elevations in the restricted zone represent energy losses through the sector gates. Table 11 outlines the statistical difference between the simulations. Each simulation was compared separately to the open boundary condition used to force the model and to the calibration model. The calibration has poor correlation to the simulations where the waterfall structure was removed because all energy was recovered from the forcing signals. Each simulation correlated very well with the respective open boundary condition, which indicates the water elevation responds rapidly to forcing from north to south. Both the signal and the individual point values follow the tidal response of the different forcing scenarios.

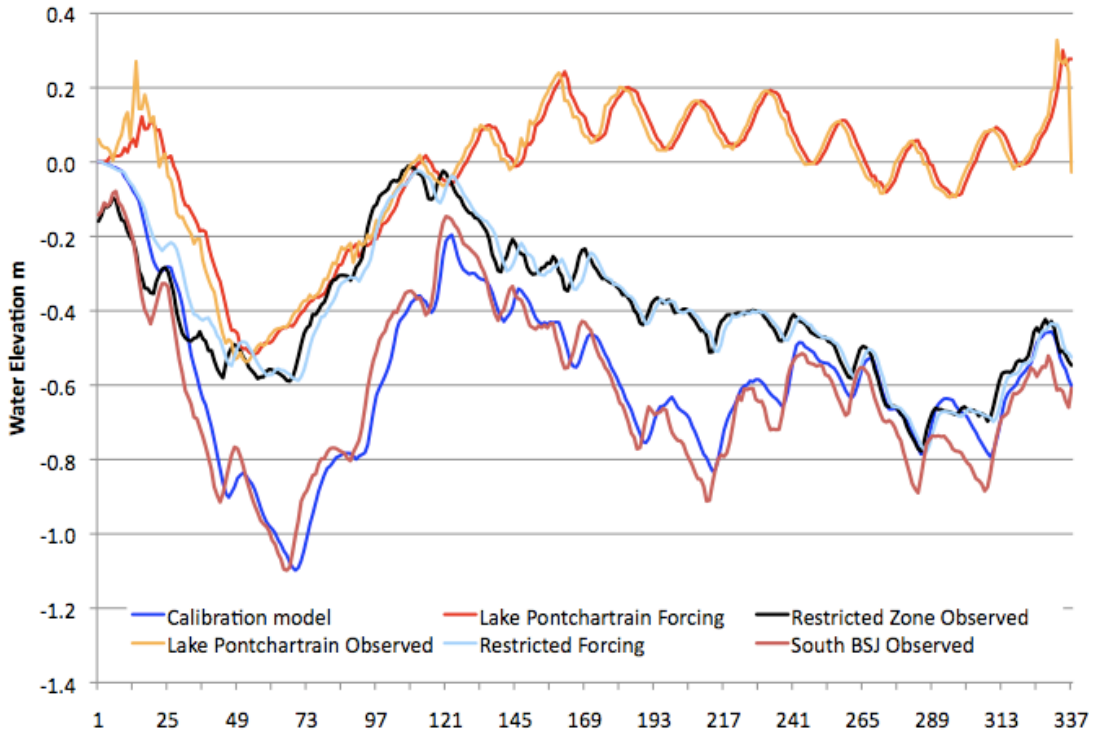

Table 11. Statistical analysis of differences between the calibration, open boundary condition or forcing, Restricted zone Forcing, and Lake Pontchartrain Forcing at the south location in Bayou St. John.

Simulation	Correlation		RME		RMSE		d	
	Forcing	Base	Forcing	Base	Forcing	Base	Forcing	Base
Base Calibration	0.95		0.05		0.07		0.97	
Restricted Forcing	0.96	0.73	0.04	0.19	0.06	0.25	0.98	0.72
Lake Pontchartrain Forcing	0.98	0.52	0.03	0.55	0.04	0.59	0.99	0.38

Figure 16. Evaluation of predicted water surface elevations at the south end of the Bayou for simulations plotted alongside observed water elevations of the inlet, Lake Pontchartrain, and North Bayou St. John.

Figure 16 shows the time dependent predicted water elevation of each simulation at the south end of Bayou St. John compared to observed water elevations from Lake Pontchartrain, the restricted zone, and south Bayou St. John. Removing the waterfall structure will allow water elevations at the restricted zone to control water elevations within the Bayou indicating control of the sector gates become more important to prevent excessive water elevations in the Bayou. BKI (2000) indicated the Bayou could be safely operated at an elevation as high as 0.27 m. The Lake Pontchartrain forcing simulation only begins to reach this elevation at the end of the simulation indicating allowing normal Lake tidal forcing to impact the Bayou will not put the local area at risk for flooding.

Salinity Simulation Results

Salinities show a similar response for both the base calibration and simulations after the waterfall is removed (Figure 17). At simulation hour 72, at the peak of the cold front, the salinities decrease in all simulations by order of decreasing water column height. The base calibration had the lowest water elevations, lowest water column height, and therefore had the lowest salinities at 2.0 ppt. The other two simulations had a similar response to the first cold front and therefore had a similar water column height that was higher than the calibration. With more depth the simulations had higher predicted salinities at 2.5 ppt at simulation hour 72. This effect shows the meteorological forcing is less effective at higher respective water elevations. All simulations continued a decreasing salinity trend as the water elevation recovered from the cold front, and the simulation with no flood control between the Lake and Bayou, Lake Pontchartrain forcing, had a more gradual trend than the other two simulations. At the north end of the Bayou the Lake Pontchartrain forcing also had the shortest acclimation period and had a good correlation to observed salinities until the cold front hit. The salinity values for all simulations stabilized after the initial decrease at a lower salinity than the observed values. The simulations with the waterfall structure removed and no flood control structures were very similar to each other while the calibration remained at a lower salinity. This data indicates the meteorological forcing at a uniform setting of 10% open water conditions overestimates some variables that impact salinity, likely precipitation, and the difference between simulations correlates to a balance between meteorological impact and water column height.

In the south location of the Bayou the calibration acclimates before the other two simulations because the calibration open boundary condition simulated the largest difference in water elevation within the first 48 hours. Both the simulation with the waterfall structure removed and the simulation with no flood control structures acclimate roughly 30 hours after the calibration. The base calibration predicted salinities show a slowly decreasing trend in the south likely due to meteorological impact. With removal of the waterfall structure and higher overall water elevations at the open boundary condition the salinities stabilize within 0.1 ppt. This indicates higher water elevations may decrease meteorological forcing. With no flood control structures the salinities rapidly diverge from the other two scenarios becoming increasingly less saline. The trend indicates the salinities of the north and south would converge under the regular tidal signal of the Lake if the simulation time had been increased another few days. The higher water elevation from Lake Pontchartrain and increased tidal signal increases transport of salinities from north to south when no flood control structures restrict flow from the Lake into the Bayou.

The far south of the Bayou has the most potential to form salinity gradients from surface to bottom because the geometry of the Bayou and distance from the open boundary restrict flow to the far south. Figure 18 shows the predicted salinity gradient between the surface and bottom of the water column for the calibration and simulation with no flood control structures at the south end of the Bayou. The simulation with no flood control structures shows a greater salinity gradient during the simulation period because the water column is higher reducing mixing at the predicted low velocities. The calibration, in contrast, has a smaller salinity gradient because both water velocity and wind have increased impact in shallow water. Figure 19 shows the predicted salinity gradient between the surface and bottom of the water column for the same scenarios but at the far south location within the Bayou. Predicted surface salinities of the far south show a similar trend as the predicted north average salinities indicating meteorological effects are important across the surface of the Bayou from north to south. Though this pattern is missing from the far south extracted data, meteorological impact is assumed to be the source of the rapid loss of salinity in the first few hours indicating the salinity loss seen at simulation hour 24 in the far south may correlate to the first few simulation hours at the south location. The far south salinity signal lacks tidal signal seen at the south location again indicating the salinity gradient is due more to meteorological forcing than to tidal transport of temperature and salinity from the open boundary.

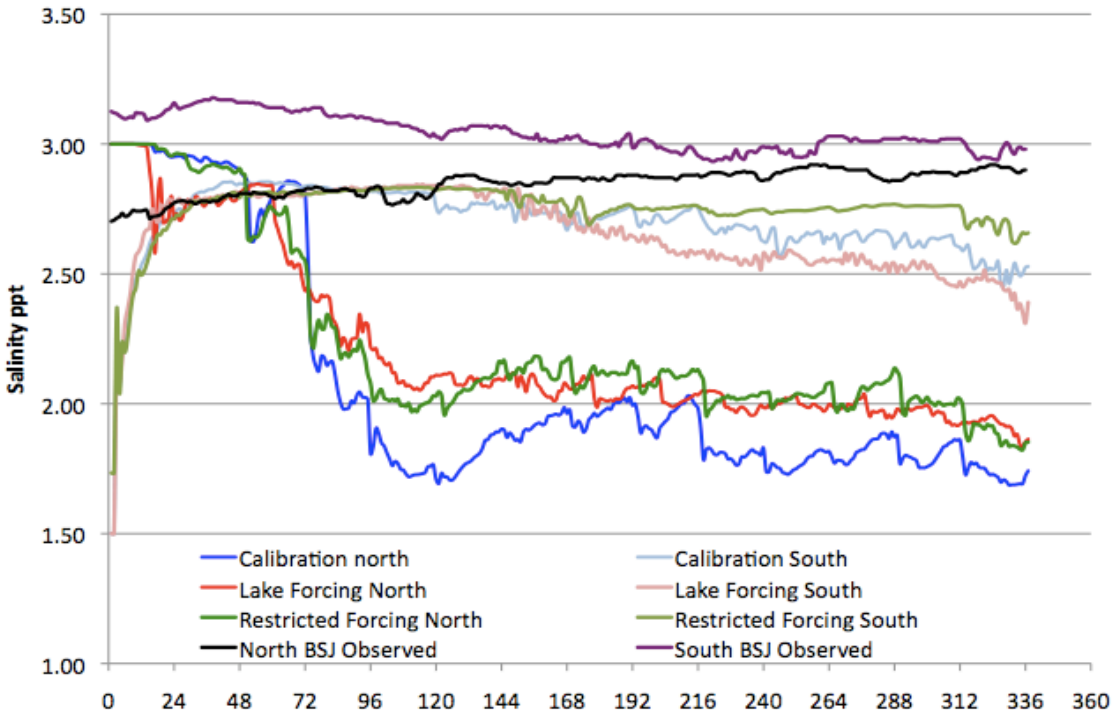

Figure 17. Time dependent salinities predicted by the calibration and simulations at the north and south end of Bayou St. John compared to observed salinities at both locations. The lighter time series represent the

south end of the Bayou and can be compared to the south Bayou observed values and the darker time series represent the north end of the Bayou and can be compared to the north Bayou observed values.

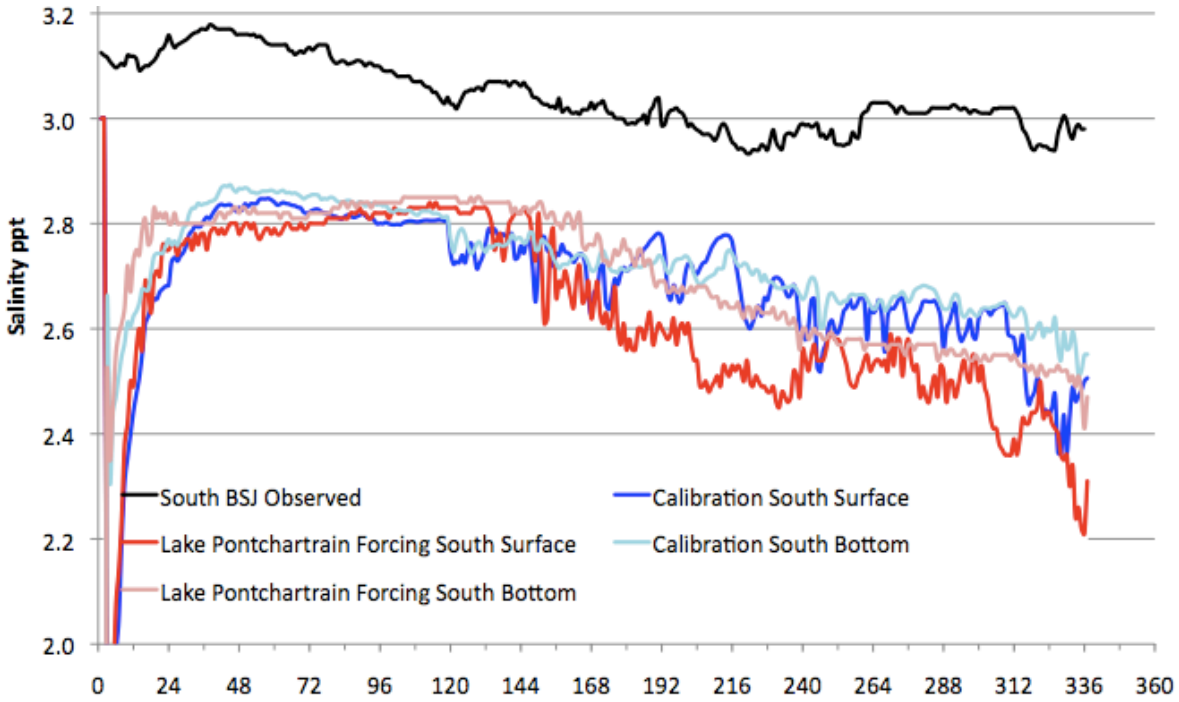

Figure 18. Time dependent salinities predicted by the calibration and the Lake Pontchartrain forcing simulation compared to the observed salinities at south Bayou St. John. The lighter time series represent bottom salinities and the darker time series represent surface salinities.

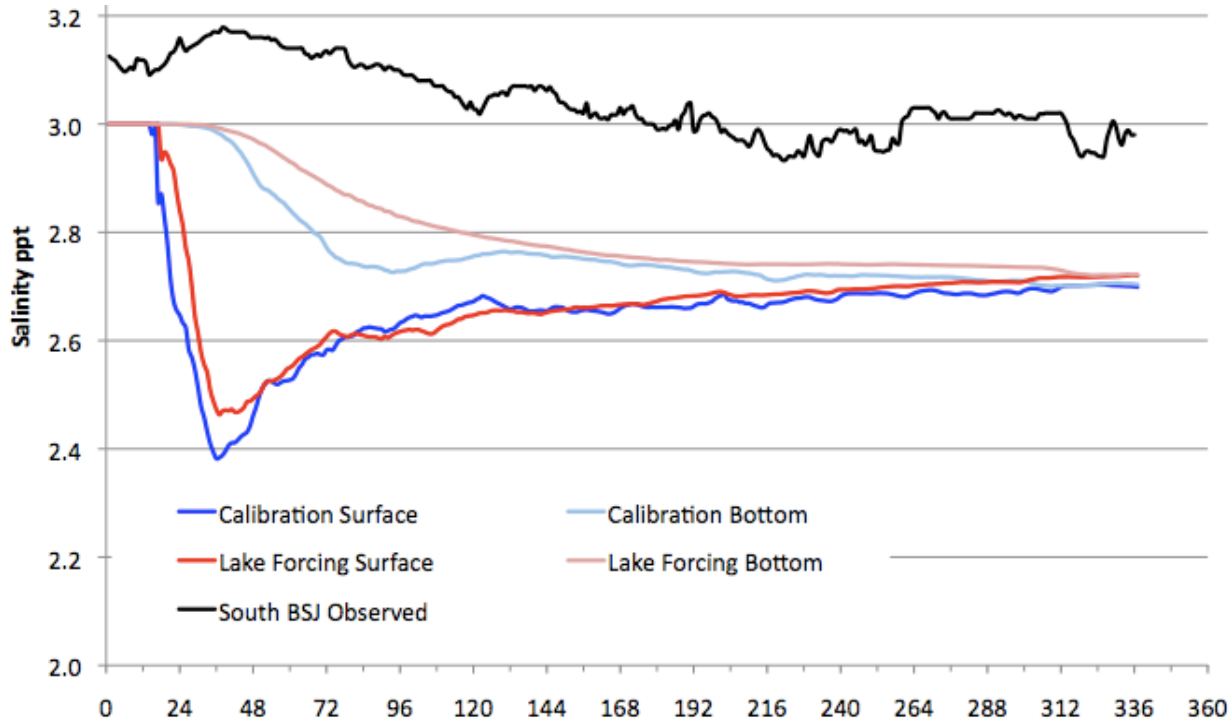

Figure 19. Time dependent predicted salinities for the far south within Bayou St. John for the calibration and Lake Pontchartrain forcing compared to observed salinities at the south end of the Bayou. The lighter time series represent the bottom salinities and the darker time series represent the surface salinities.

Temperature Simulation Results

Temperature analysis reveals a similar pattern to salinity with respect to acclimation time and ordering of simulations. Figure 20 shows the time dependent predicted temperatures for the calibration and simulations for the north and south end of the Bayou in comparison to observed temperatures at the same locations. The acclimation period for each respective location is the same as seen in the salinity profiles. Temperatures extracted at the north end of the Bayou for each simulation have a predicted maximum of 1°C heat loss from the observed temperature at that location. Salinity and temperature have the same pattern for both the north and south locations indicating the cooling mechanism is the same driver that lowers salinity, which is likely precipitation. Water temperature values drop much faster than the water elevation and corresponding temperature signal at the inlet. The temperature and salinity of Bayou St. John would follow the trend of these qualities at the open boundary condition if water from the inlet controlled temperature and salinity in the Bayou. The lack of agreement between the temperature signal in the Bayou and temperature signal at the open boundary also points to meteorological forcing as the main driver of temperature.

The order of simulations with respect to temperature trends is also the same as seen with salinity. Lower overall water elevations lead to lower temperatures in the north due to increased

meteorological impact on shallow water. In the south the simulation for removal of the waterfall structure maintained a high temperature above the calibration as the water height buffered meteorological impact and the simulation with no flood control structures had a decreasing trend that would converge with the north temperatures if the trend continued during additional simulation hours.

The far south has the highest predicted temperatures and highest salinities of any location due to increased distance from the inlet, depressed flows, and shallow nature of the narrow southern section. The predicted surface water temperature in the far south is slightly lower than the bottom as seen in Figure 21 for the simulation with no flood control structures. A similar pattern is seen at slightly different values for the other two simulations. The forced temperature tidal signal at the open boundary is predicted at the north and south but is not predicted in the narrow southern section indicating this section of water does not respond to tidal forcing and meteorological forcing may control density gradients at this location. The north surface and bottom temperatures respond to forcing within 48 hours of simulation time, the south surface and bottom temperature respond to forcing after 120 to 150 hours of simulation time, but the far south does not respond during this simulation (Figure 21).

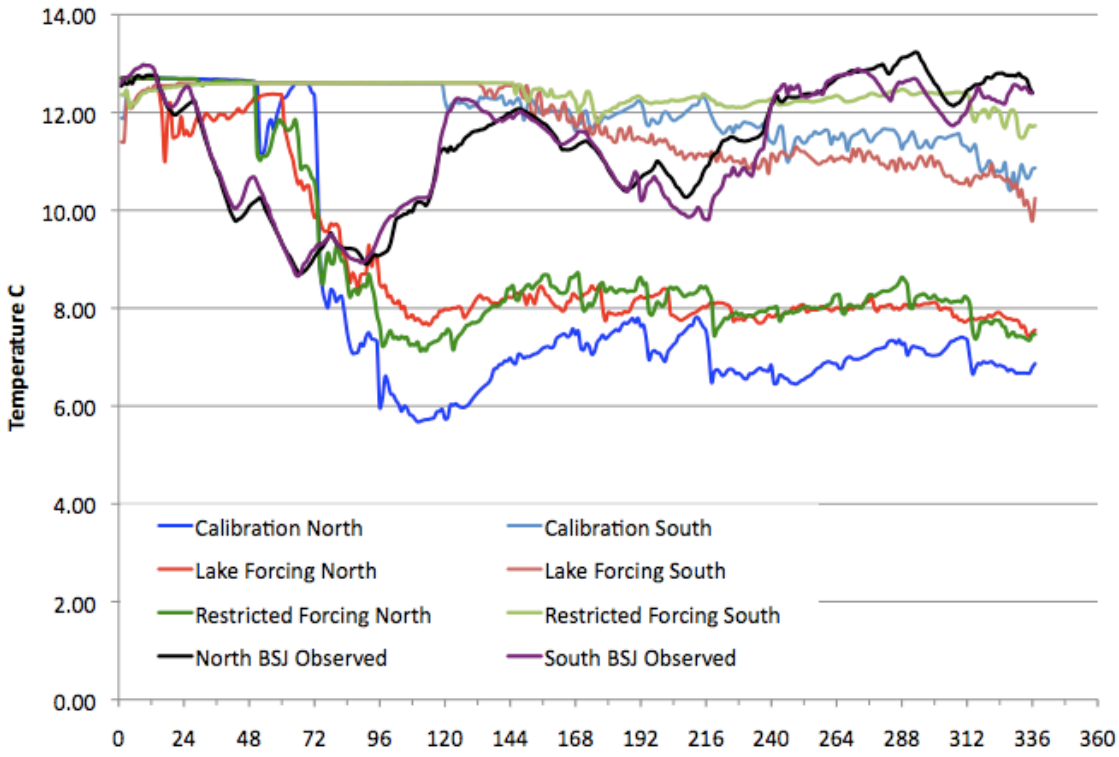

Figure 20. Analysis of temperature for simulations 1 through 4 showing the north, south, and far south locations with reference to the inlet salinities

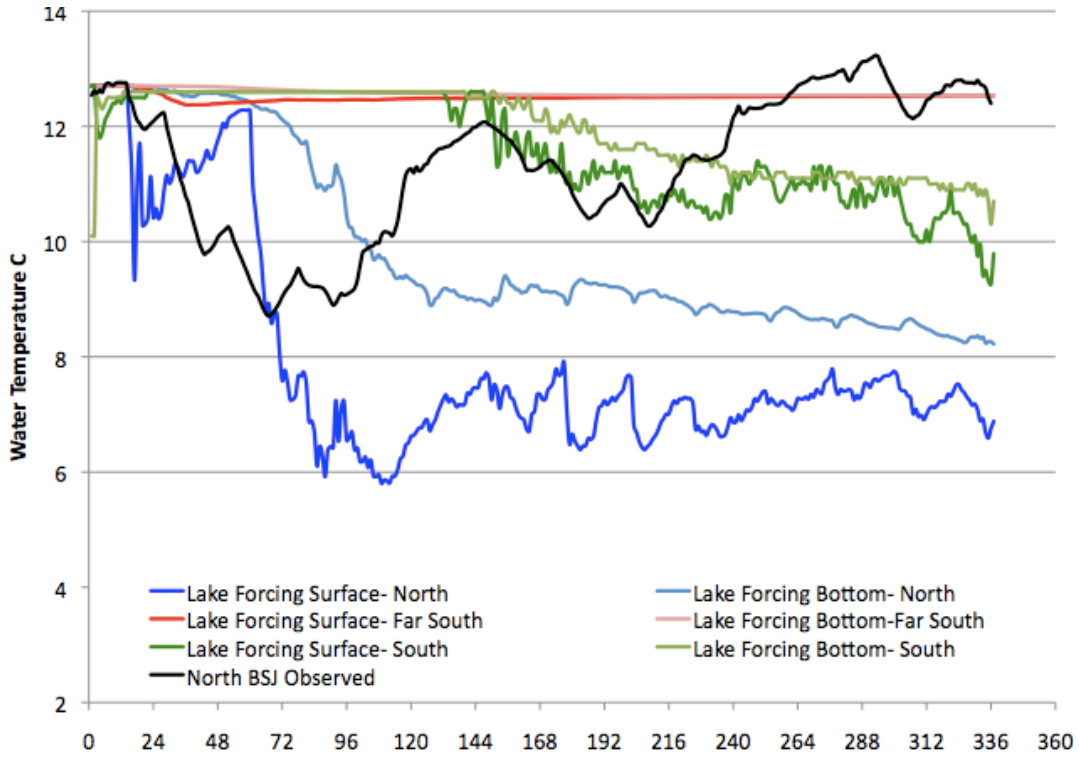

Figure 21. Time dependent predicted temperature comparison of surface and bottom temperatures for the Lake Pontchartrain forcing simulation from north to far south. The blue time series represent the north, the green time series represents the south, and the red series represents the far south

Mixing and Tidal Exchange Flow Simulation Results

Mixing and tidal exchange flow can be used to evaluate the changes in hydraulic characteristics during various forcing simulations. Stratification at all extracted locations was maintained throughout the simulation period, though the temperature and salinity trends towards convergence shown above indicate stratification would be diminished if the simulation had continued another few days. Low velocity in the far south again attributes to the high-predicted values for the bulk Richardson numbers at the all locations more than density gradients.

Though all simulations showed high bulk Richardson numbers, the difference in values from north to south changed among the models due to changes in velocities as well as slight changes in density gradients. Figure 22 shows the time dependent, predicted bulk Richardson number for the simulation with no flood control structures between the Lake and Bayou from north to far south as daily moving averages and Figure 23 shows the same data for the calibration. The simulation of the removal of the waterfall structure had a response intermediate to these two simulations. Both simulations show increasing stratification with increasing distance to the south. The simulation with no flood control structures shows the north bulk Richardson numbers have a signal that is unique to the south and far south because flow losses occur at the Mirabeau and Filmore Avenue

bridges, which lie between the north and south location. A similar pattern is observed for the calibration. However, with no flood control structures the south and far south bulk Richardson numbers have a good correlation. This is due to the similarity in density gradient between the two locations before the south location begins to respond to tidal forcing and indicates the velocity losses are linear between the two locations. There are no physical restrictions between the north and south only curvilinear Bayou geometry and bottom friction, so a linear loss of velocity is not unreasonable. A similar patter is observed for the calibration where the south and far south have the some correlation until the south begins to respond to tidal forcing at approximately 144 simulation hours. The south predicted bulk Richardson numbers have a decreasing trend after beginning to respond to tidal forcing due to increased velocities. The far south predicted bulk Richardson numbers also show a decreasing trend later in the simulation at approximately 204 simulation hours. This could indicate the far south begins to respond to tidal forcing during the calibration, but the far south in the simulation with no flood control structures does not respond during the simulation period. The calibration has the largest fluctuations in water elevation while the simulation with no flood control structures has higher water elevations but smaller fluctuations in water elevation. The relative stability of Lake Pontchartrain does not appear to activate mixing in the narrow southern section of the Bayou based on bulk Richardson numbers.

Tidal exchange flow was evaluated at the north, middle and south sections of the Bayou, and was compared between simulations to investigate if a change would occur as a result of removal of the flood control structures. The along-Bayou component of the velocity was laterally averaged, along with an average depth along each of the four transect. Flow was converted so that positive flow is to the south (or into the Bayou) while negative flow is to the north (or out of the Bayou). Flows in all simulations were similar during the first cold front at the south location as shown in Figures 24 and 25. This is expected because both the Lake Pontchartrain signal and the Inlet signal (from the restricted area) decreased to the same water surface elevation at a similar rate during the first cold front and rose to a similar water elevation after the front passed. This is reasonable indicating that even without flood control structures similar oscillations at the Lake would produce somewhat similar exchange flows and flushing within the Bayou. The flow signals for the calibration and simulation with the waterfall structure removed are in phase while the signal the simulation with no flood control structures is out of phase with the calibration. The sector gates and a sand bar lie between the restricted zone and Lake Pontchartrain. These two impediments both cause energy loss into the restricted zone represented by lower water elevations and attenuated tidal signal represented by the phase differences in the signals.

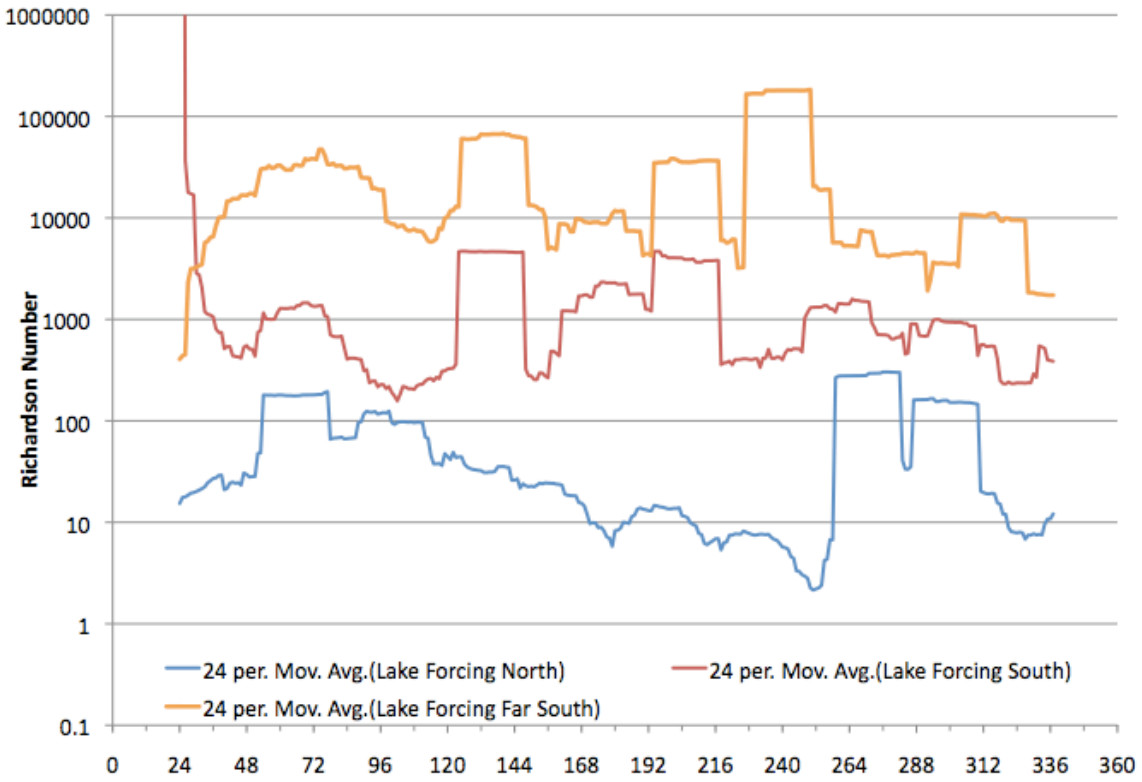

Figure 22. Bulk Richardson number evaluation through Bayou St. John from north to far south. Vertical stratification is observed only for the far south locations indicated by red boxes.

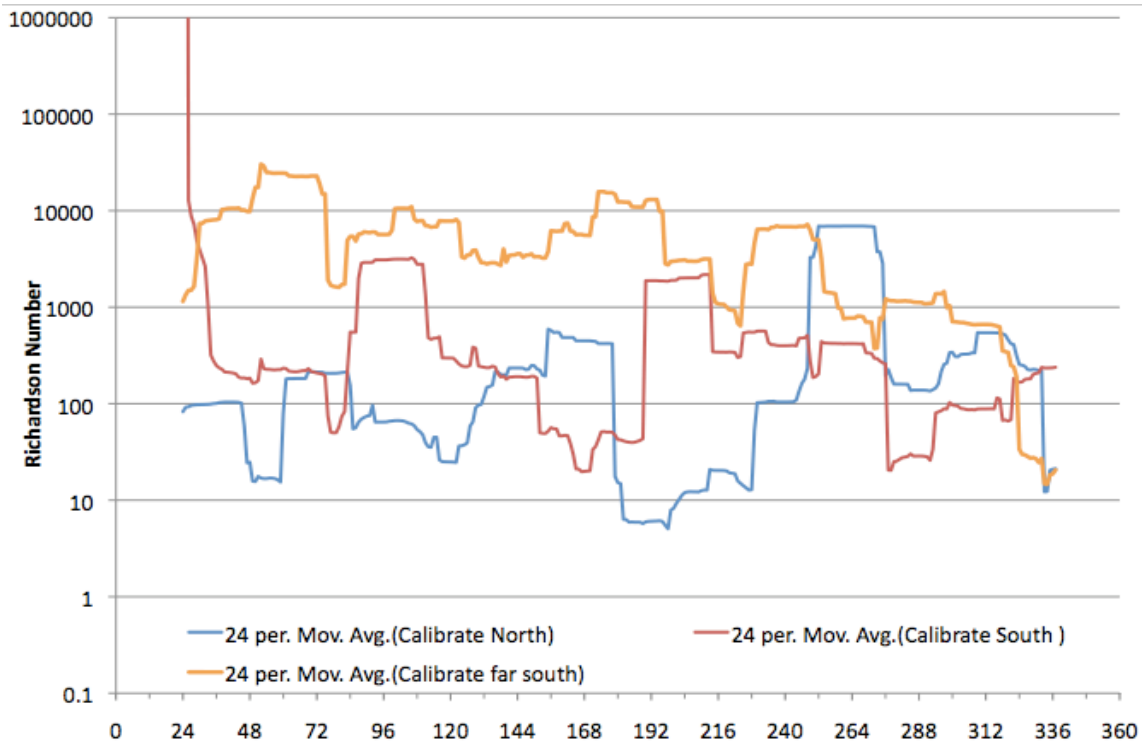

Figure 23. Bulk Richardson number evaluation from north to south within Bayou St. John in reference to the calibration.

Predicted flows for once the waterfall structure is removed begin to diverge from the calibration after simulation hour 96 and flows with no flood control structures begin to diverge after simulation hour 50. The simulation with the waterfall structure removed continues to follow the calibration signal closely but shows a marked decrease in flow magnitude for flow south and slightly higher magnitude for flow north. This is due to a slightly different nature of the forcing; for instance the calibration has sudden increases in flow to the south that are short in duration with longer periods of low flow back to north while the simulation with the waterfall structure removed has a more even distribution of north and south flow with a magnitude of approximately 0.7 m^3/s at the south end of the Bayou (Figure 24). Energy loss through the waterfall structure does not attenuate the tidal signal as significantly as the structures between the restricted zone and Lake Pontchartrain. Flows predicted using no flood control structures begin to stabilize once higher water elevations are established and maintained at the open boundary. Lake Pontchartrain tidal signal has a stronger astronomical signature marked by diurnal oscillations which produces a more even distribution of north and south flow from approximately 0.5 to -0.5 m^3/s at the south end of the Bayou and only exceeds this range due to climatic events such as a cold front (Figure 25).

Tidal exchange flow across the Bayou from north to the far south shows a large loss in flow magnitude (Figures 26, 27, and 28). The Bayou becomes narrower and shallower with increasing distance from the north. In addition, there are several bridge crossings that would further impede flow by dissipating energy and attenuating flow as a result of a tidal or frontal response. The calibration had the highest flows due to having larger water elevation oscillations and therefore a more energetic forcing signal. Removal of the waterfall structure also diminished the magnitude of the changes in water elevation as did using Lake Pontchartrain water elevations as a boundary condition. Despite have a higher water elevation and therefore a larger tidal prism, these two scenarios had lower overall velocities that resulted in lower flows. In the far south location the calibration simulation produced a maximum instantaneous flow of 0.75 m^3/s, the simulation removing the waterfall structure produced a flow of 0.7 m^3/s, and the flow during the simulation with no flood control structures was 0.7 m^3/s.

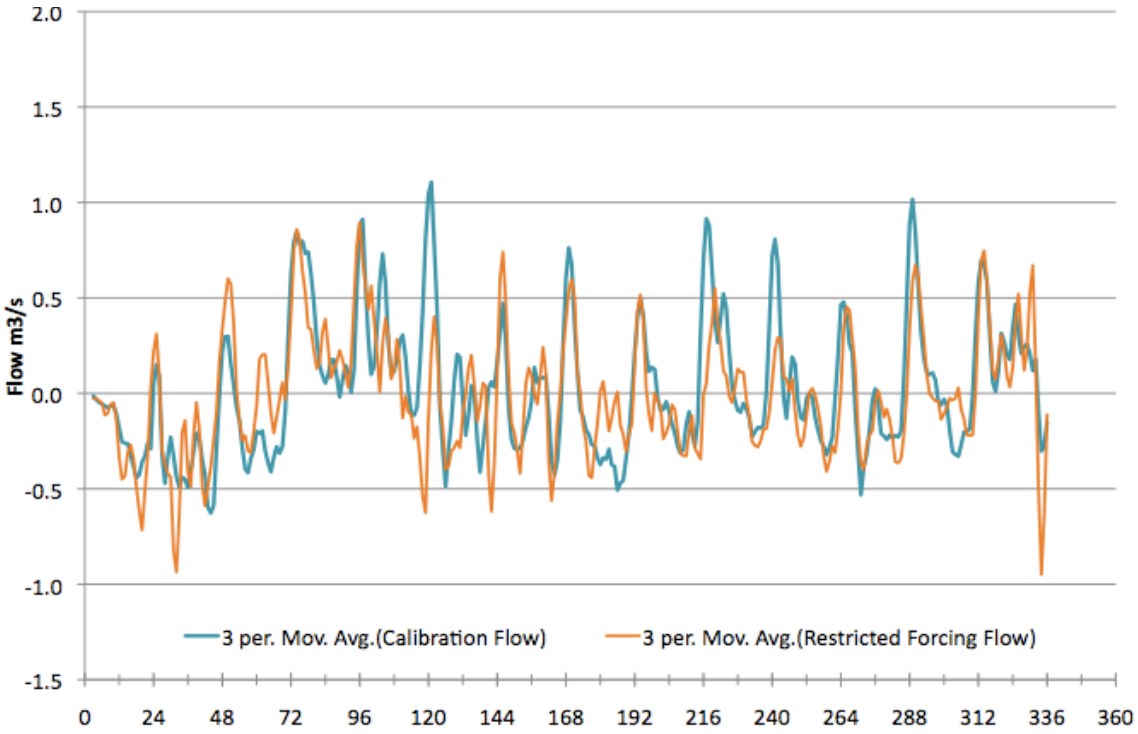

Figure 24. Predicted time dependent flow through Bayou St. John for the calibration compared to Lake Pontchartrain forcing at the south location.

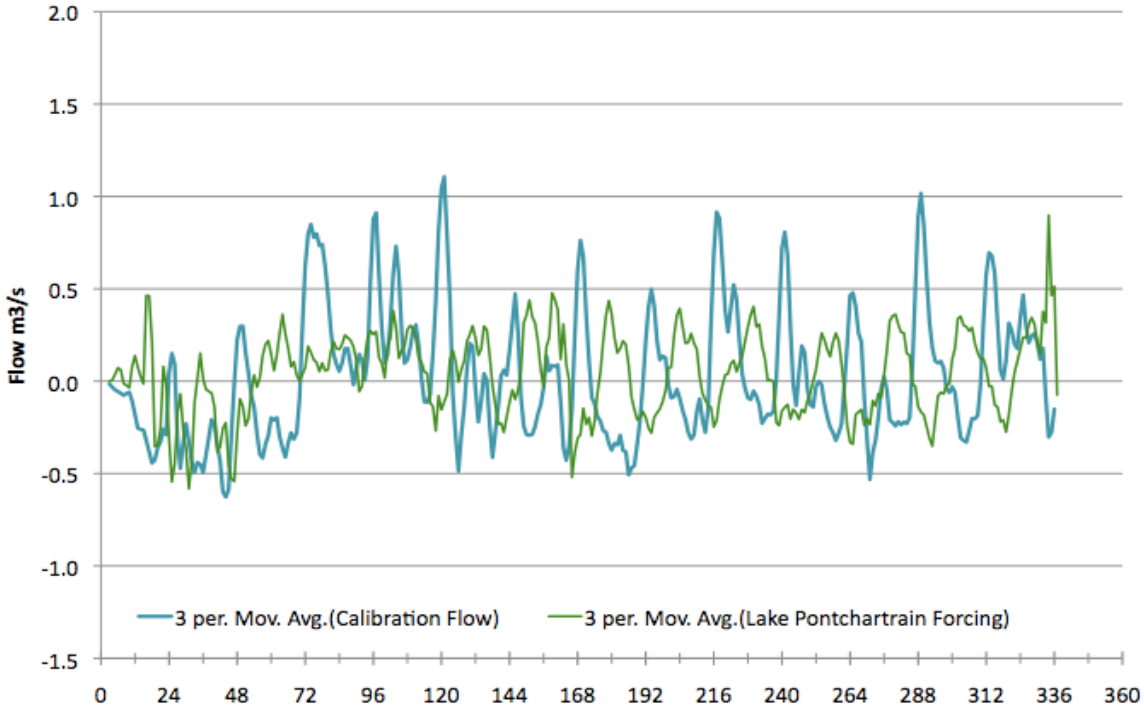

Figure 25. Predicted time dependent flow through Bayou St. John for the calibration compared to Restricted zone forcing at the south location.

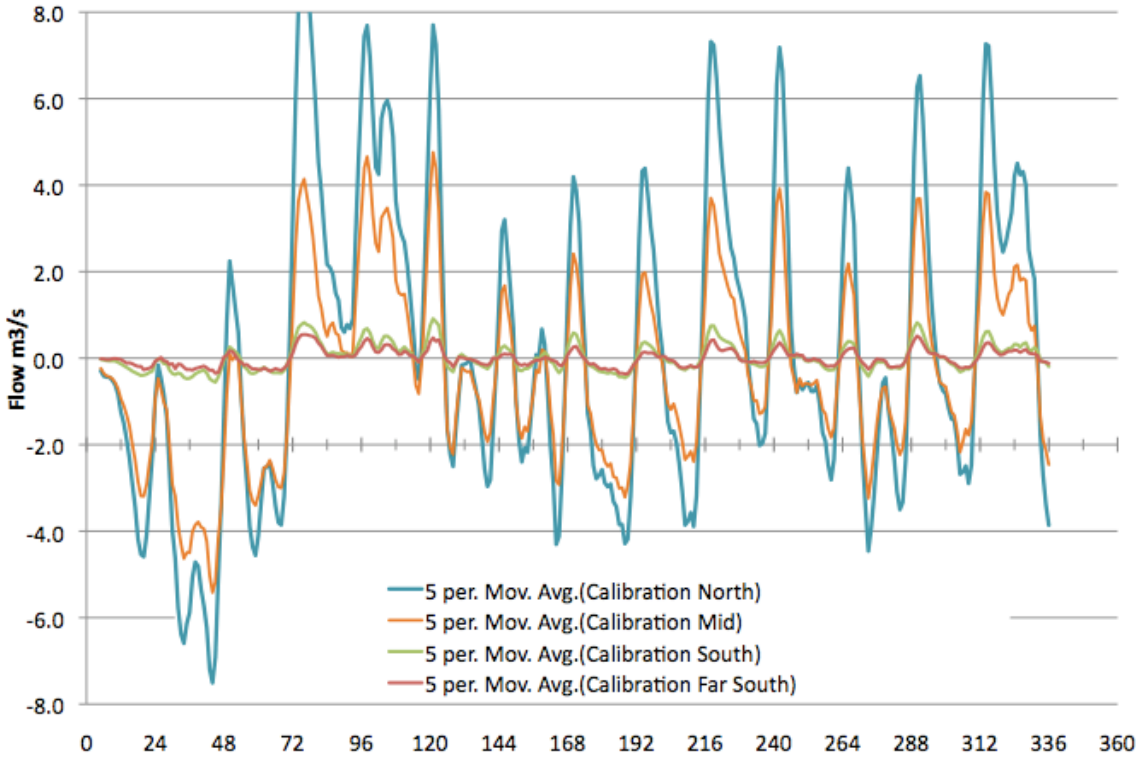

Figure 26. Time dependent flow for the Calibration forcing simulation from north to south showing flow dissipation with increasing distance from the open boundary.

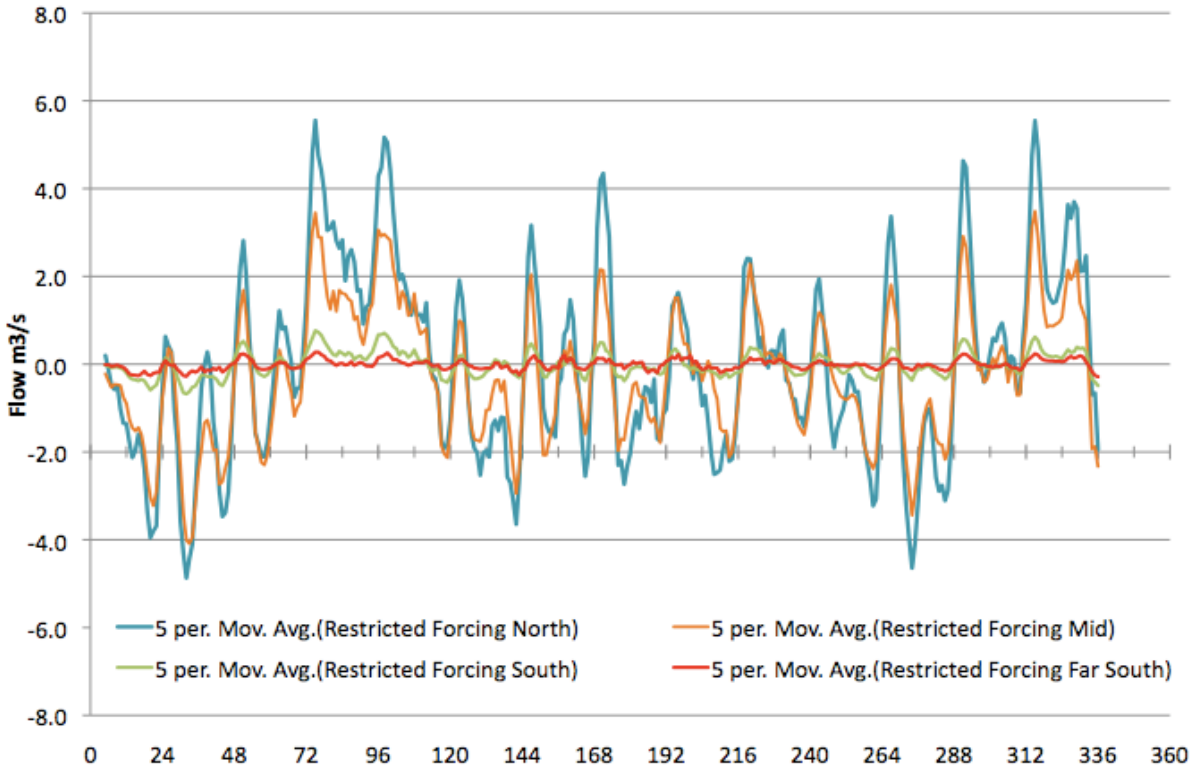

Figure 27. Time dependent flow for the Restricted zone forcing simulation from north to south showing flow dissipation with increasing distance from the open boundary.

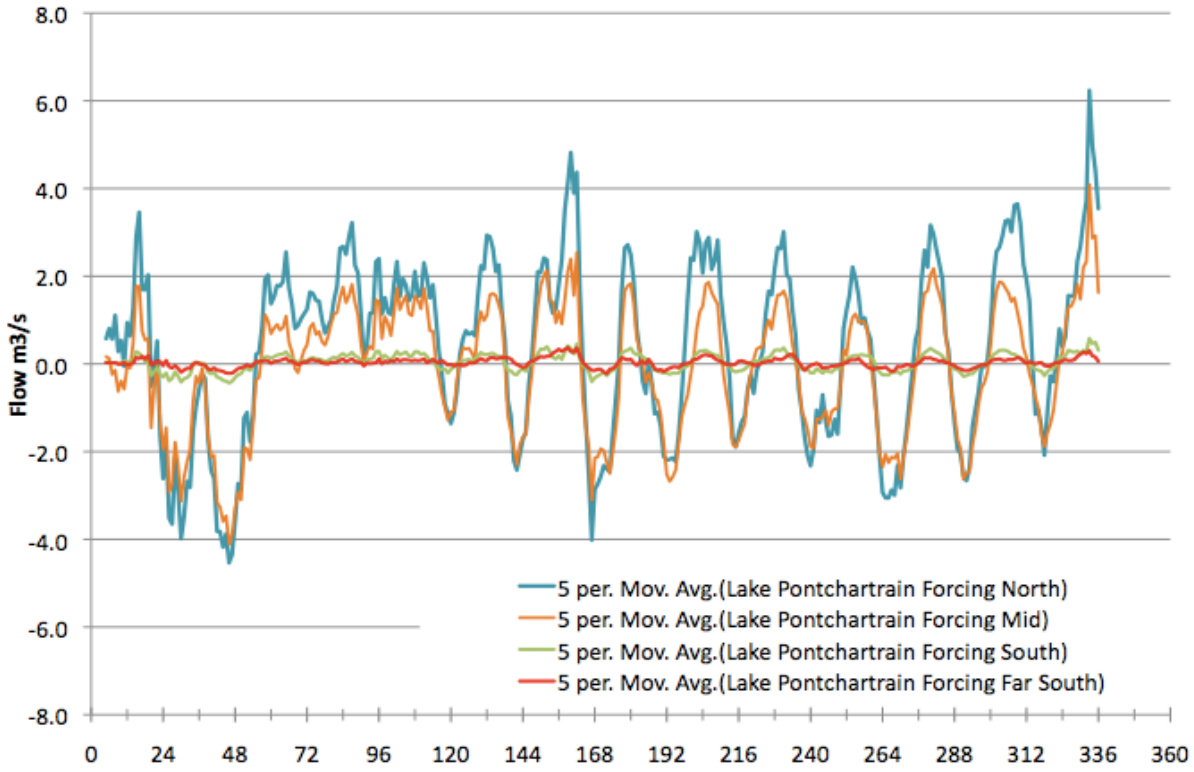

Figure 28. Time dependent flow for the Lake Pontchartrain forcing simulation from north to south showing flow dissipation with increasing distance from the open boundary

Figures 26 through 28 show the loss of flow from north to south. The diurnal tidal signature of the Lake is predicted at both the south and far south sections of the Bayou though flow does not significantly change between simulations. The loss of flow between the different simulations is due to the variability in water elevations alone for each forcing dataset. The waterfall structure causes water elevations to decrease to an elevation lower than the other simulations then increase to an elevation similar to the restricted zone once the water equilibrates across the structure. A similar loss of energy across the waterfall structure is observed several times during the simulation period causing this forcing signal to have large water elevation amplitudes. Flows in the far south have a predicted range of -0.5 to 0.7 m^3/s for the calibration and a maximum range of -0.4 to 0.7 m^3/s for both of the other simulations. The simulation after removing the waterfalls structure has the same range of flow magnitudes as the simulation with no flood control structures. However, the simulation with no flood control structures has a more robust astronomical signature while the signal from removing the waterfall structure is less predictable and appears to have a secondary dependency (likely the presence of the waterfall structure). Water will back up behind the waterfall structure causing the energy losses seen in this dataset to be exaggerated and

unpredictable. Once the waterfall structure is removed the energy losses will be solely attributable to the sector gates and the sand bar. The Lake tidal signal, on the other hand, is well documented and very predictable giving flood control operators a basis for water elevation control once the waterfall structure is removed.

Shear Stress Simulation Results

Shear stress is proportional to the square of the velocity, and therefore the simulations with the highest velocities have proportionally highest shear stress values, however shear stress did not exceed the critical threshold of 0.1 N/m^2 (Haralampides, 2000) for any of the simulations. Bridge constrictions reduce tidal flow exchange but increase velocities through the restricted area. Figure 28 shows the predicted relative shear stress values during the restricted zone forcing simulation at the Mirabeau and Filmore Ave. bridge constrictions. Though the predicted shear stress at the bridge restrictions represent the highest shear stress values in the model, these values do not approach the critical value for sediment resuspension.

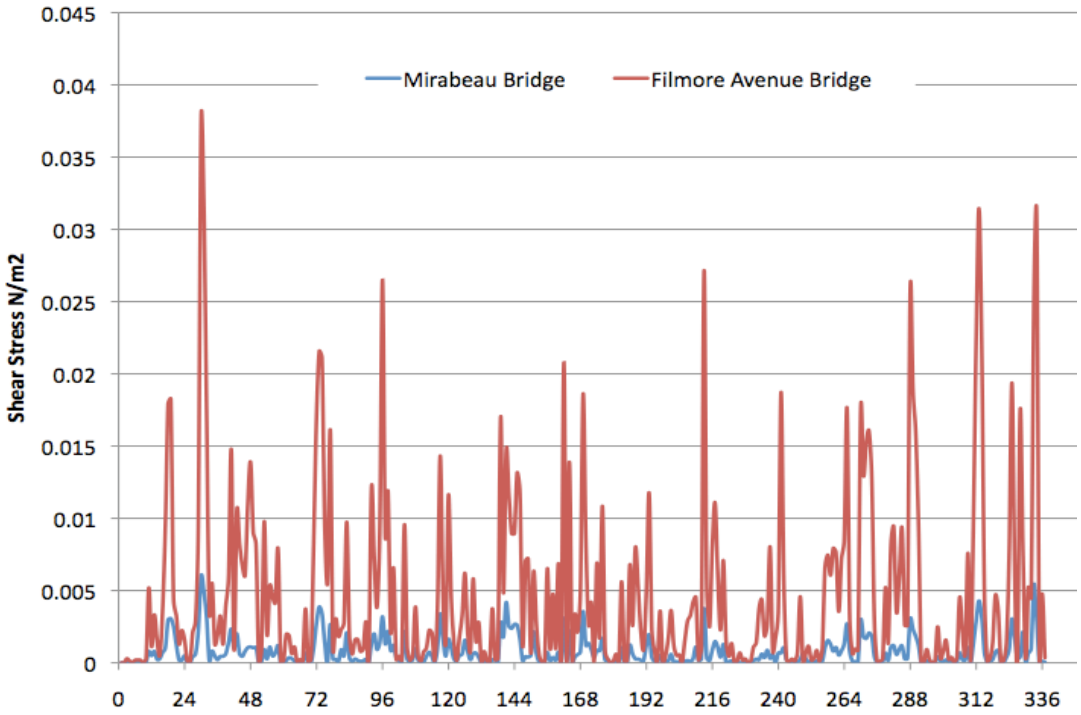

Figure 29. Time dependent shear stress values for the Restricted zone forcing simulation extracted in the center of each restriction caused by Mirabeau and Filmore Ave bridges.

Chapter 6. Discussion

Evaluation of Hypothesis 1

The first hypothesis for this study stated the increased tidal mixing in Bayou St. John after the removal of the waterfall structure will increase tidal exchange flow resulting in temperature and salinity values to more closely follow Lake Pontchartrain values. The first hypothesis was proven false due to the loss of tidal exchange flow from north to south when the waterfall structure was removed for this simulation due to a loss in the magnitude of water elevation oscillations. Tidal exchange flows from the simulation with no flood control structures also showed a loss of flow despite higher water elevations, but the salinity and temperature values in the south began to converge with the north values indicating flushing. The regular tidal signal from Lake Pontchartrain in addition to higher water volumes allowed progressive flushing of temperature and salinity from north to south. Though the simulation period ended before the entire southern tail was flushed, the trend in the simulation indicates the entire bayou would benefit from opening the sector gates to allow Lake Pontchartrain water elevations and tidal signal to impact the Bayou. Therefore, despite the rejection of the first hypothesis with data for the current simulation period, sustained water elevations and a constant tidal signal in Bayou St. John due to operation of the sector gates will proportionally increase flushing if the waterfall structure was removed.

All simulations showed that water elevations at the north and south were very similar indicating the Bayou quickly equilibrates. The tidal exchange flow was reduced from north to south due to localized restrictions and because the Bayou becomes increasingly narrow from north to south. Discrepancies in temperature, salinity, and model response time from north to south all indicate the tidal exchange flow is greatly reduced from north to south. All locations north of the SWB valve located just south of I-610 responded to the boundary forcing of temperature and salinity for both the calibration and when the waterfall structure was removed, though as the Bayou narrows the response becomes more delayed due to reduced tidal exchange flow. The simulation with no flood control structures in place was the only simulation that showed flushing of salinity and temperature past I-610 into the narrow southern tail. The predicted values of both temperature and salinity were overall lower than observed values at the north end of the Bayou. This result is likely due to an overestimation of precipitation into the Bayou. Bayou St. John is a shallow water body and therefore is highly susceptible to climatic influences. Precipitation in south Louisiana is high and though all meteorological forcing was reduced to 10% open water conditions,

precipitation can still have a significant impact on the model. Uniform application of meteorological conditions appears to be unrealistic for this location, though precipitation appears to be driving temperature and salinity more than other meteorological forcing. Wind speeds above what was used in this study could additionally induce setup at the south location and account for the observed differences in water elevation from the north and south locations. Summer atmospheric heat will amplify the stratification from north to south due to higher heat export and generally lower wind speeds. Evaporation will also increase during the summer. Areas of the Bayou that are narrow and shallow will be more susceptible to meteorological effects compared to the wider and deeper sections at the north end of Bayou St. John.

Bulk Richardson numbers indicate the Bayou St. John remains relatively stratified (although stratification is rather weak) except during high velocity events at the north end of the Bayou. This pattern emerges due to the very low velocities predicted throughout the Bayou, which drive the bulk Richardson numbers exponentially higher when velocities approach zero. This suggests that even low flows activated from north to south in the Bayou will have a large impact on water quality; a small increase in water velocity will balance any stratification that is present through longitudinal and vertical mixing.

Evaluation of Hypothesis 2

The second hypothesis states that removing the waterfall structure will increase bottom shear stress thereby leading to sediment resuspension, which will redistribute contaminated sediment in Bayou St. John. Having this sediment redistributed into the otherwise healthy ecosystem in the northern portion of Bayou St. John has the potential to degrade the health of the ecosystem, contaminate the wildlife through biomagnification, and eventually endanger the health of the local fisheries. This hypothesis is also false because the waterfall structure was not found to have any significant impact on shear stress values compared to the critical threshold. The lack of potential resuspension and transport agrees with previous reports of sediment contamination (Mowat and Bundy, 2001) that suggest contamination accumulates in the southern tail of Bayou St. John due to runoff at the southern end. The lack of resuspension predicted in this study indicates the contamination will not be redistributed through the Bayou.

The C_d value used in this project was based on previous work due to the anticipated high drag caused by the shallow nature of the bathymetry, the presence of cypress stumps etc., all of which increase drag. However, this value ($C_d \sim 0.01$) could be much lower if only grain roughness is considered ($C_d \sim 0.005$). This would contribute to even lower potential shear stress or higher

(should a higher drag be selected), which would yield a proportionally higher shear stress. However the drag coefficient would have to be 100 times higher before the shear stress values exceed the critical threshold in the open sections of the Bayou. At localized bridge restrictions the drag coefficient would only need to double to bring shear stress values close to the critical threshold. Higher velocities could also increase shear stress in the Bayou, which may occur if the waterfall structure is removed and a large change in water elevation is observed at the inlet either due to climatic influence or opening the sector gates when water levels are low in the Bayou.

Conclusions

The waterfall structure causes large energy losses from the inlet into Bayou St. John as was captured by direct field observations. Once this structure is removed the water elevation within the Bayou will quickly equilibrate to water elevations within the inlet. The field measurements of water elevation do not indicate how the inlet will react once the waterfall structure is removed. The back up of water upstream of the Bayou due to limited flow through the waterfall structure may have caused some of the tidal attenuation observed between Lake Pontchartrain and the inlet. Once the waterfall structure is removed the inlet water elevations may be in phase with Lake Pontchartrain tidal signals, likely increasing flow exchange for each tidal and meteorological event.

When the Bayou was open to Lake Pontchartrain temperature and salinity transport was increased from the north to south. Both the temperature and salinity in the north section of the Bayou were reduced at the onset of the model and, once the southern section began to respond to the forcing, both salinity and temperature began to reduce at that location as well. If the simulation with no flood control structures had been continued for another few days both temperature and salinity at the north and south sections of the Bayou would have converged. This pattern was only predicted for the simulation with no flood control structures indicating both a higher water volume and a regular tidal signal applied for an extended period of time (more than 14 days) is required to transport temperature and salinity into the southern zone of the Bayou.

Lake Pontchartrain water elevations could directly impact the Bayou with more aggressive operation of the sector gates as suggested by the BKI report (2000) once the waterfall structure is removed. Some tidal attenuation is anticipated through the narrow inlet, however the energy loss will be minor compared to the current flood control strategy. There are a couple of considerations for sector gate control that would improve water quality in the Bayou: 1) the difference in water elevation across the sector gate immediately prior to opening will directly effect tidal exchange flow and shear stress in the north section of the Bayou; 2) the longer the sector gates are left open the

more likely Lake driven temperature and salinity will travel to the southern end of the Bayou. Increasing tidal exchange flow will allow the sector gates to be opened for a shorter period of time, however the associated increased shear stress has the potential to mobilize contaminants that directly affect the ecological health of the Bayou. Opening the sector gates for a longer period of time negates the need for a large change in water elevation to exist immediately prior to opening the gates and has the highest likelihood of flushing the Bayou. These considerations assume the prior standing order to keep the Bayou at a low water elevation of -0.8 m (NAVD88) no longer applies. With the waterfall structure removed maintaining a water elevation at -0.8 will require limiting flows through the sector gates to a level similar to the current restrictions provided by the waterfalls structure, which will negate any positive impact removing this structure is meant to achieve. The data in this study shows that removing the waterfall structure allowed the Bayou water elevation to increase by 0.16 m, while opening the sector gates allowed the water elevation to increase by an additional 0.56 m. However, the water elevation even under Lake Pontchartrain forcing increased the Bayou water level to a maximum of 0.29 m NAVD88. This maximum is just above 0.27 m NAVD88, which was suggested by BKI (2000) to have little impact on the local area due to the current height of the levees. A new safe operating water elevation should be established for the Bayou that reflects the recovered energy anticipated after the waterfall structure is removed in order to allow the Bayou to benefit from the increased tidal forcing.

Finally, the contaminated sediments in the narrow southern end of the Bayou are not likely to be resuspended or transported under normal Lake Pontchartrain or inlet forcing. This means the contamination will continue to accumulate in this section of the Bayou and continue to adversely impact the local ecology through leaching of toxins into the water and preventing a benthic community from establishing in the sediment. These sediments should be remediated in order for a healthy benthic community to establish in the sediments. Additionally, measures should be taken to prevent urban run-off from entering the Bayou such as installing best management practices or diverting the run-off to storm water treatment facilities. Though temperature and salinity will define species richness and diversity (BKI, 2000), the sediment contamination levels are currently damaging the ecological health of the Bayou.

Future Recommendations:

Producing a viable model for Bayou St. John was a challenge due to the numerous unknown variables. Several assumptions were made to compensate for the unknowns. This included meteorological forcing, including evaporation and precipitation, selection of a bottom roughness height, and drag coefficient used in the shear stress equation. This model contrasted the model

designed by BKI (2000) in that the Bayou was allowed to interact with several components of meteorological forcing, including heat flux and evaporation, and evaluated the internal dynamics of temperature, salinity, tidal exchange flow, and shear stress. The models presented here bypassed controls at the sector gates to focus on downstream impacts of water elevation changes and hydraulic characteristics. Water elevation changes were based on direct field observations within Bayou St. John opposed to assumed anthropogenic control. Future models should concentrate on delineating the unknowns, which include accurate bathymetric data, drag coefficients, accurate footprint and elevation of the sand bar at the entrance to the Sector gates, and operations data for sluice gate control and distal discharge. Sediment transport was not modeled during this study, however the potential for sediment transport within the north Bayou corridor could alter the local bathymetry and possibly increase Lake-borne contamination.

Higher water elevations in the Bayou predicted with the removal of the waterfall structure will top the growth on the "algal" weir currently controlling flow into the city park Lakes, and therefore a valve may be required at this location in the future. As shown, Bayou St. John is a small basin and therefore responds rapidly to changes at the inlet and in Lake Pontchartrain. Sector gate operations previously used to control water elevations will prove inadequate once the waterfall structure is removed, particularly if the goal is to keep the Bayou water elevation at -0.8 m NAVD88 (BKI, 200). The algal weir is also an important water control structure that could be used to control water velocities in the Bayou by dampening large water fluctuations from Lake Pontchartrain if a better control structure was installed.

The critical shear stress threshold of the bottom sediment used in analysis here is based on measurements of critical shear in Lake Pontchartrain. Though this is a reasonable first estimate of the geophysical characteristics in Bayou St. John, a more detailed analysis of the sediment should be conducted to verify or change this parameter specifically looking at water saturation of the sediments. In addition, the contamination data used here are sparse with only one data point per bridge crossing. A more comprehensive sampling grid is required to delineate the areal extent of the contamination as well as the depth of penetration in south Bayou St. John. Furthermore, contamination is assumed to be accumulated over long time periods, however sampling runoff into the Bayou from various bridges should be used to quantify the input contamination to supplement transport potential of soluble contaminants and the rate of accumulation in the sediment.

Future models with the above considerations will greatly add to the understanding of the ecology and hydraulic response in Bayou St. John. Additional field data will be required to develop an inlet model that can robustly predict hydrodynamics near the entrance to the Bayou.

References:

Blumberg, A.F. and G.L. Mellor. (1987) "A description of a three-dimensional coastal ocean circulation model" in Three dimensional coastal ocean models. Ed. N.S. Heaps. AGU, Washington, D.C. 1-16.

Boyd, G.R., J.M. Palmeri, S. Zhang, and D.A. Grimm. (2004) Pharmaceuticals and personal care products (PPCPs) and endocrine disrupting chemicals (EDCs) in stormwater canals and Bayou St. John in New Orleans, Louisiana, USA. Science of the Total Environment. 333: 137-148.

BKI. (2000) Bayou St. John water management study. Hydrologic, hydraulic, ecological, and water quality. Prepared for the Commissioners of the New Orleans Levee Board. 89pp.

Brogan, S. (2010) Red drum (Sciaenops ocellatus) habitat use in an urban system; behavior of reintroduced fish in Bayou St. John, New Orleans. Thesis. University of New Orleans. 72pp.

Carnelos, S. (2003) Fate of pathogen indicators in the stormwater runoff. Ph.D. Dissertation, Dept. of Civil and Environmental Engineering, University of New Orleans, New Orleans, LA

Cheng, N. (1997) Simplified settling velocity formula for sediment particle. Journal of Hydraulic Engineering. February 1997:149-152.

Chaiworapuek, W. (2007) The engineering investigation of the water flow past the butterfly valve. Thesis. The College of the Holy and Undivided Trinity of Queen Elizabeth. Dublin, Ireland. 64pp.

Chilmakuri, C. (2005) Sediment transport and pathogen indicator modeling in Lake Pontchartrain. Dissertation. University of New Orleans. New Orleans, LA. 156pp.

Dortch, M.S., M. Zakikhani, S. Kim, and J.A. Steevens. (2008) Modeling water and sediment contamination of Lake Pontchartrain following pump-out of Hurricane Katrina floodwater. Journal of Environmental Management 87.3: 429-442.

EBI. (2011) Citizens guide to environmental investigation and public prosecution. Energy Probe Technical Bulletin. Toronto, Ontario.

FitzGerald, D.M., I.V. Buynevich, R.A. Davis Jr., and M.S. Fenster. (2002) New England tidal inlets with special reference to riverine-associated inlet systems. Geomorphology. 48.1-3: 179.

Flocks, J., J. Kindinger, M. Marot, and C. Charles. (2009) Sediment characterization and dynamics in Lake Pontchartrain, Louisiana. Journal of Coastal Research. 54: 113-126.

Fontenot, L.R. (2004) An evaluation of reference evapotranspiration models in Louisiana. Thesis. University of New Orleans. New Orleans, LA. 83pp.

Georgiou, I. and J.A. McCorquodale. (2007) Final Report: Rapid prototyping of NASA MODIS 250m data in the calibration/validation of a sediment transport model for water quality assessment and public health decision support. Technical Report. University of New Orleans, New Orleans, LA. 32pp.

Gerritsen, F., D.W. Dunsbergen, and C.G. Israel. (2003) A rational stability approach for tidal inlets, including analysis of the effect of wave action. Journal of Coastal Research. 19: 1066-1081.

Glenn, S.M. and W.D. Grant. (1987) A suspended sediment stratification correction for combined wave and current flows. Journal of Geophysical Research. 29(C8):8244-8264.

Gonzales, C., M.K. Smith, H.W. Mielke, and F.P. Kale. (1997) Trace metals in sediment, soils, and water of urban Bayou Saint John and rural Jean Lafitte National Park, Louisiana. Fundamentals in Applied Toxicology. 36:278.

Haralampides, K. (2000) A study of the hydrodynamics and salinity regimes of the Lake Pontchartrain system. Dissertation. University of New Orleans. New Orleans, LA. 219pp.

Hench, J.L., B.O. Blanton, and R.A. Luettich Jr. (2002) Lateral dynamic analysis and classification of barotropic tidal inlets. Continental Shelf Research. 22:2615-2631.

Houck, O.A., F. Wagner, and J.B. Elstrott. (1989) To restore Lake Pontchartrain, A report to the Greater New Orleans Expressway Commission on the sources, remedies, and economic impacts of pollution in the Lake Pontchartrain Basin. Metairie, LA. 270pp.

Hsu, S.A., J.M. Grymes, and Z. Yan. (1997) A simplified hydrodynamic formula for estimating the wind-driven flooding in the Lake Pontchartrain-Amite river basin. National Weather Association Digest. 21:4.

LPBF. Lake Pontchartrain Basin Foundation. (2006) Comprehensive Management Plan. Metairie, LA., Lake Pontchartrain Basin Foundation.

Li, C., E. Weeks, and B.W. Blanchard. (2010) Storm surge induced flux through multiple tidal passes of Lake Pontchartrain estuary during Hurricanes Gustav and Ike. Estuarine, Coastal, and Shelf Science. Article in Press, xxx:1-9.

List, J.H., and R.P. Signell. (1996) Modeling the long-term climate of near-bottom orbital velocity in the Lake Pontchartrain Basin. USGS open-file report. 96-xxx.

Manheim, F., L. Hayes, and A. McIntire. (1998) Lake Pontchartrain Basin: Bottom sediments and regional scientific and educational resources. USGS Open-File Report 98-805.

Martinez, L., S. O'Brien, and S. Brogan. (2008) Bathymetric survey of Bayou St. John. Internal report. University of New Orleans. New Orleans, LA. 5pp.

Mariotti, G., S. Fagherazzi, P.L. Wiberg, K.J. McGlathery, L. Carniello, adn A. Defina. (2010) Influence

of storm surges and sea level on shallow tidal basin erosive processes. J. of Geophysical Research. 115(C11012): 1-17.

McCorquodale, J.A., D. Moulton, D. Barbé, Y. Wang, K. Haralampides, and S. Carnelos. (2001) "Reliability of NPDES derived loads in urban runoff." In: *Urban drainage modeling, proceedings of the Specialty Symposium of the World Water and Environmental Research Congress*. Eds. R.W. Brashear and C. Maksimovic. ASCE. Reston, VA. 301-12.

McCorquodale, J. A., I. Georgiou, S. Carnelos, and A. J. Englande. (2004) Modeling coliforms in storm water plumes. Journal of Environmental Engineering & Science 3.5: 419-431.

McNeil, J., C. Taylor, and W. Lick. (1997) Measurements of erosion of undisturbed bottom sediments with depth. Journal of Hydraulic Engineering. June 1996:316-324.

Mellor, G.L. and T. Yamada. (1982) Development of a turbulence closure model for geophysical fluid problems. Revisions in Geophysical Space Physics. 20:851-875.

Mowat, F.S., and K.J. Bundy. (2001) Correlation of field-measured toxicity with chemical concentration and pollutant availability. Environmental International. 27:479-489.

Pardue, J.H., W.M. Moe, D. Mcinnis, L.J. Thibodeaux, K.T. Valsaraj, E. Maciasz, I. van Heerden, N. Korevec, and Q.Z. Yuan. (2005) Chemical and microbiological parameters in New Orleans floodwater following Hurricane Katrina. Environmental Science and Technology. 39(22):8591-8599.

Ranasinghe, R. and C. Pattiaratchi. (2003) The seasonal closure of tidal inlets: causes and effects. Coastal Engineering Journal. 45(4):601-627.

Roberson, J.A., J.J. Cassidy, and M.H. Chaudhry. Hydraulic Engineering. Houghton Mifflin Co. One Beacon St. Boston, MA. 662 pp.

Schindler, J. (2009) Bayou St. John water quality study. Personal communication. October 21, 2010.

Signell, R.P. and J.H. List. (1997) Modeling waves and circulation in Lake Pontchartrain. Gulf Coast Assoc. Geol. Soc., Trans. 47: 529–532.

Smith, P. (2011) unpublished data.

Stanev, E.V., M. Dobrynin, A. Pleskachevsky, S. Grayek, and H. Günther. (2009) Bed shear stress in the southern North Sea as an important driver for suspended sediment dynamics. Ocean Dynamics. 59:183-194.

Stone, J.S., W.A. Subra, and P.J. Minvielle, (1972) Surface circulation of Lake Pontchartrain: A wind dominated system. Final Report. Gulf South Research Institute, Proj. NS-255. 122 pp.

Traynum, S. and R. Styles. (2008) Exchange flow between two estuaries connected by a shallow tidal channel. Journal of Coastal Research. 24(5):1260-1268.

Uncles, R.J. and J.A. Stephens. (2011) The effects of wind, runoff and tides on salinity in a strongly tidal sub-estuary. Estuaries and Coasts. 34:758-774.

van der Wegen, M., A. Dastgheib, and J.A. Roelvink. (2010) Morphodynamic modeling of tidal channel evolution in comparison to empirical PA relationship. Coastal Engineering. 57:827-837.

Wang, G., H.W. Mielke, V. Quach, C. Gonzales, and Q. Zhang. (2004) Determination of polycyclic aromatic hydrocarbons and trace metals in New Orleans soils and sediments. Soil and Sediment Contamination. 13:313-327.

Ward, K.A. (1982) Ecology of Bayou St. John. Thesis. University of New Orleans, Print.

Willmott, C.J., S.G. Ackleson, R.E. Davis, and J.J. Feddema. (1985) Statistics for the evaluation and comparison of models. Journal of Geophysical Research. 90(C5):8995-9005.

Work, P.A., J. Guan, E.J. Hayter, and S. Elci. (2001) Mesoscale model for morphologic change at tidal inlets. Journal of Waterway, Port, Coastal, and Ocean Engineering. September/October: 282-289.

Appendix X- Relative Positioning of Sample Locations and Boundaries in Bayou St. John

Site Name	Easting	Northing
YSI deploy 1	781357.80	3324820.02
YSI deploy 2	781308.69	3324625.69
YSI deploy 3	781085.36	3321529.20
Aquadop deploy	781308.69	3324625.69
City Park Weir	781103.31	3323160.05
City Park Pump 1	780854.85	3320805.72
City Park Pump 2	780689.91	3320458.79
S&WB Valve 1	781100.41	3321463.56
S&WB Valve 2	780669.64	3319393.59
Waterfall Inflow	781346.00	3324706.54
SS-1	781272.22	3324150.38
SS-2	781166.57	3323439.60
SS-3	781154.54	3322903.03
SS-4	781143.08	3322366.47
SS-5	781179.97	3321855.09
SS-6	780965.52	3321123.19
SS-7	780948.92	3320190.55
SS-8	780954.27	3319989.37

Vita

The author was raised in Eliasville, TX and attended school in Graham, TX. She graduated a year early from high school in May 2001 and continued her higher education at Texas A&M University at Galveston. In December 2005, she graduated with a BS in Marine Biology. In Fall 2005 she was accepted into the LSU Department of Geology as a Research Assistant under Dr. Annette Engel where she completed the equivalent of an undergraduate degree in geology courses and attended geology field camp. In August 2010 she transferred to the UNO Department of Earth and Environmental Science to complete a MS in Hydrogeology under Dr. Ioannis Georgiou.